10 YEARS ANNIVERSARY

INORGANIC CHEMISTRY

FRONTIERS

REVIEW

Check for updates

Opportunities and challenges in aqueous nitrate and nitrite reduction beyond electrocatalysis

Guanling Yang,[a,c] Pengfei Zhou,[a,c] Jinsheng Liang,[a,c] Hao Li [iD] *[b] and Fei Wang [iD] *[a,c]

Nitrate (NO_3^-) and nitrite (NO_2^-) ions are common health-threatening contaminants in water. To reduce nitrate and nitrite, catalytic thermal reduction using molecular hydrogen as the reducing agent is a strategy with some clear advantages. However, this method is relatively less explored, with some vital open questions still to be addressed. In this paper, we review the current stages of thermal nitrate and nitrite reduction on the aspects of catalyst synthesis, mechanistic insights, reaction activity, product selectivity, design guidelines for promising catalysts, and the efficiency comparison between thermal and electrocatalytic reduction. The main opportunities and challenges of this thermal reduction method in drinking water and wastewater treatment are discussed. Moreover, in addition to discussing this reaction's typical N_2 formation selectivity, we also discuss the possibility of forming ammonia by tuning the reaction selectivity *via* rational catalyst design. This review shows that in addition to the currently popular electrocatalytic nitrate reduction, scientific efforts should also be devoted towards the thermal reduction of nitrate and nitrite. We hope that this review will arouse more interest from the catalyst community to explore the mechanistic insights and design guidelines for thermal nitrate and nitrite reduction.

1. Introduction

Surface and groundwater pollution has attracted broad attention in recent years, while nitrate (NO_3^-) is one of the most concerning pollutants.[1] As a health-threatening pollutant, NO_3^- accounts for ~70% of the groundwater samples and is ~13 times more frequent than other contaminants.[2] Generally, the level of NO_3^- in nature is relatively low, but human activities (*e.g.*, septic systems, animal husbandry, and farming) have dramatically increased the NO_3^- concentration.[3–7] When ingested, NO_3^- can easily be reduced *in vivo* to nitrite (NO_2^-), which can cause methemoglobinemia (the so-called "blue-baby syndrome").[8] NO_2^- can react with amines and amides in the gastrointestinal tract to form carcinogenic N-nitroso compounds.[3,5,7,9] In addition, long-term exposure to low-concentration NO_3^-/NO_2^- may cause various cancers,[7] which is one of the reasons why NO_3^- and NO_2^- have become serious contaminants in water treatment. The maximum contaminant levels (MCLs) of NO_3^- and NO_2^- have been set at 10 and

1.0 mg N L^{-1}, respectively (calculated from the nitrogen weight, denoted as mg N L^{-1}), by the United States Environmental Protection Agency (US EPA).[10] The European Drinking Water Directive has set concentration limits for NO_3^- and NO_2^- at 11.3 and 0.15 mg N L^{-1}, respectively.[11] Besides, the World Health Organization guideline values of NO_3^- and NO_2^- are 11.3 and 0.91 mg N L^{-1}, respectively.[12]

Some wastewater treatment methods have been applied for NO_3^- and NO_2^- removal, such as electrodialysis,[13] reverse osmosis,[14] ion exchange,[15] and biological treatment.[16] However, the main drawbacks and challenges of these methods have been reported, as summarized in Table 1. When NO_3^-/NO_2^- is treated with adsorbents or reverse osmosis membranes, it leads to the accumulation of contaminants on the adsorbent surface and in the permeate wastewater, for which secondary treatment with high-concentration NO_3^-/NO_2^- is required. Biological nitrification can convert NO_3^-/NO_2^- to harmless N_2, but it takes a long operation time.[16] In terms of biological treatment, microorganisms can contaminate pure water to some extent. Moreover, the microbial reaction is temperature-dependent, and the reactivity is significantly lower in winter when the temperature is low.[17] Among various treatment technologies, electrocatalytic processes show great potential for NO_3^-/NO_2^- removal but have some significant disadvantages, including the addition of electrolytes and chloride ions, and the need to maintain a high pH, which greatly limits their widespread use. In addition, the generally

[a] Key Laboratory of Special Functional Materials for Ecological Environment and Information (Hebei University of Technology), Ministry of Education, Tianjin 300130, China. E-mail: wangfei@hebut.edu.cn
[b] Advanced Institute for Materials Research (WPI-AIMR), Tohoku University, Sendai 980-8577, Japan. E-mail: li.hao.b8@tohoku.ac.jp
[c] Institute of Power Source and Ecomaterials Science, Hebei University of Technology, Tianjin 300130, China

4610 | *Inorg. Chem. Front.*, 2023, **10**, 4610–4631

This journal is © the Partner Organisations 2023

Table 1 Descriptions of various nitrate treatment methods.[17] Copyright 2003, Elsevier. Note: the data and content of the table are from ref. 17 by Centi and Perathoner

Method	Ion exchange	Reverse osmosis	Biological denitrification	Electrocatalytic reduction	Thermal catalytic reduction
Fate of nitrate	Adsorbed	Concentrated	N_2	N_2 and NH_3	N_2 and NH_3
Waste	Waste brine	Waste brine	Bacteria sludge	Waste brine	None
Chemical additives	Sodium chloride	Sulfuric acid alkali	Ethanol and phosphoric acid	Electrolytes	H_2
Percentage of efficiency	85–98%	75–80%	98%	98%	100%
Flexibility in variable	Medium	Medium	Low	Medium	High
Energy use	Low	High	Medium	High	Low
Space	Limited	Limited	High	Limited	Limited
Movable	Yes	Yes	No	Good	Yes
Manageability	Good	Good	Poor	Good	Good
Type of operation	Periodic regeneration	Continuous	Continuous	Continuous	Continuous
Sensitivity to deactivation	Medium	High	High	High	High
Automatic control	Simple	Simple	Complex	Simple	Simple
Start-up time	Immediate	Immediate	Up to 1 month	Immediate	Immediate
Monitoring required	Little	Little	Intensive	Little	Little
Selectivity of the process	Low	Low	High	High	High
Odors	No	No	Yes	Yes	No
Noise	Some	High	No	No	No

high overpotentials will lead to various side reactions and corrosive gases during electrolysis, which may corrode the electrodes and limit the energy utilization efficiency.[18,19]

Thermal catalytic reduction of nitrate and nitrite by hydrogenation is an alternative beyond electrocatalysis. This technique was first systemically studied in 1989 as a promising method for nitrite removal.[20] The main reason why thermal catalysis stands out among many chemical treatments is its high hydrogen utilization rate and the high selectivity for harmless N_2. The H_2 used in thermal catalytic reduction can be obtained by the electrolysis of water using renewable energy sources (*e.g.*, wind and solar). The reduction of nitrate by noble metal catalysts in the liquid-phase usually proceeds in two steps: (1) reduction of nitrate to nitrite and (2) reduction of nitrite to N_2 or NH_3/NH_4^+. Nitrite reduction was found to be a structure–sensitive reaction during the reaction catalyzed by Pt–Cu bimetallic catalysts, while nitrate reduction to nitrite was found to be a structure-insensitive process.[21–23] Meanwhile, related studies have shown that the selectivity of N_2 during the reaction on the catalyst is determined by the reduction of NO_2^-, and the toxicity of nitrate in water is mainly from NO_2^-.[24] For this reason, an in-depth understanding of the reaction process of nitrite reduction and the corresponding catalyst design is essential. This is one of the main reasons why a comprehensive review of thermal catalytic nitrate and nitrite reduction is urgently needed.

Based on the statistical analysis of previous publications (Fig. 1), most of the research focused on the electrocatalytic reduction of nitrate, while there were fewer studies involving nitrite reduction or thermal reduction, of which there were very few studies on the thermal reduction of nitrite. Unlike the research hotspot, electrocatalytic nitrate reduction,[25] the

thermal reduction of nitrate and nitrite is much less studied, and thus its importance is generally dismissed. In this review, we provide comprehensive discussions on thermal nitrate and nitrite reduction on the aspects of catalyst synthesis, mechanistic insights, reaction activity, product selectivity, design guidelines for promising catalysts, and the efficiency comparison between thermal and electrocatalytic reduction.

2. Discussion

2.1. Reaction process

2.1.1 Catalyst synthesis. In previous reports, nitrate and nitrite reduction catalysts were synthesized by a variety of methods, including precipitation,[26] plasma spraying,[27] sol–gel synthesis,[28] impregnation,[26] and microwave-assisted synthesis.[29] However, we note that the synthesis of nitrate and nitrite reduction catalysts is not limited to the methods described above; any kinds of synthetic methods that can lead to the formation of effective catalysts that are stable under experimental operating conditions (*e.g.*, room temperature, aqueous phase, and reducing environment) are worthy of being tested with thermal nitrate and nitrite reduction.[30] Because the synthetic methods are beyond the scope of this review, we do not focus on the details of catalyst synthesis.

2.1.2 Chemical reactor. To test the catalytic reduction activity of different types of catalysts for nitrate and nitrite reduction in aqueous solution, many experiments were performed in intermittent[31–35] and semi-intermittent reactors.[36–40] The main reason was that intermittent or semi-intermittent reactors have advantages such as operational flexibility, variable throughput, low investment, and quick start-up.

This journal is © the Partner Organisations 2023

Inorg. Chem. Front., 2023, **10**, 4610–4631 | **4611**

Fig. 1 Statistical summary of the number of publications reporting electrocatalytic and thermal reduction of nitrate and nitrite. Source: Web of Science.

However, for continuous operation and process scale-up analysis, fixed-bed and trickle-bed continuous reactors are required.[41–44] For instance, Chinthaginjala *et al.*[42] studied the effects of the catalyst particle size through a fixed-bed reactor. Pd catalysts supported on carbon-nanofibers (CNFs) were synthesized *via* Pd colloids stabilized with polyvinyl-alcohol (PVA). Pd catalysts with a narrow particle size distribution and an average Pd size between 2.6 and 30 nm were immobilized on CNFs. The prepared catalysts were then tested for thermal nitrite reduction in water, with the turnover frequency (TOF) found to be independent of the Pd size. However, the selectivity of ammonia decreased significantly with an increase in Pd size.[42] Slurry or fixed-bed reactors operating in the batch or semi-batch mode are diffusion-limited because of the low solubility of hydrogen in water as well as the limited accessibility of hydrogen to the catalyst surface. Therefore, catalytic membrane reactors (Fig. 2a and b) were proposed as an alternative to overcome previous drawbacks and improve the performance of nitrate reduction. A tubular catalytic reactor with a catalyst film is shown in Fig. 2c.[45–48] This reactor establishes an effective contact between different phases (hydrogen, aqueous nitric acid solution, and the catalyst), thereby tuning up the nitrite reduction performance. The reactor plays a key role in promoting the conversion rate of nitrite. Reactor design has advanced considerably in the last decade, but there is still much room for improvement to accommodate more types of catalysts.

2.2. Reaction mechanism

In terms of the reaction mechanism, herein, we first discuss the catalytic reduction of nitrate to nitrite. Thermal reduction of nitrate to nitrite requires a metal that can activate H_2 (*e.g.*,

Pd or Pt) and a promoter metal (*e.g.*, In, Sn, or Cu) to help reduce nitrate to nitrite. The promoter metal itself usually cannot dissociate H_2, and it uses the spilt hydrogen from Pd (or Pt) to facilitate nitrate reduction (Fig. 3a).[51–53] Previous studies provided experimental observations that in the presence of some special elements as the promoters (*e.g.*, In, Cu, or Sn), nitrate reduction to nitrite is facile and not rate-limiting, in contrast to the more sluggish subsequent reduction of nitrite to N_2 or NH_3/NH_4^+.[54] However, many promoters do not continue the reduction of nitrite. Although some studies have discussed the unique role of In as a promoter for nitrate reduction,[55] the reason why these promoters can only reduce nitrate to nitrite is not clear and remains an open question.

In nitrate and nitrite reduction, the rate-determining step usually exists in nitrite reduction.[56] Therefore, we focus more on the mechanism of thermal catalytic reduction of nitrite to N_2/NH_3, which was derived from previous combined theoretical and experimental studies (Fig. 3b). Firstly, H_2 (after H–H activation) is used as a reducing agent to reduce nitrite to NO*, which is a proven highly spontaneous redox reaction. Subsequently, NO* can dissociate to form N* or form NOH*/HNO* by hydrogenation.[57] Due to the multiple available hydrogenation pathways, there are at least five pathways for NH_3/NH_4^+ formation (Fig. 3b, green pathways). In contrast, N_2O^* formation from N* is a proven key step in N_2 formation.[57] Shin *et al.* found that N_2O^* can be formed *via* the reaction of N*, H*, nitrite, and water, in good agreement with experimental observations.[15] Subsequently, N_2O^* is rapidly consumed to form N_2^*.[58,59] In conclusion, it can be seen from Fig. 3b that there are at least five possible pathways for the formation of NH_3/NH_4^+ and only two pathways for N_2. However, N_2 formation is usually thermodynamically more favorable.[36]

4612 | *Inorg. Chem. Front.*, 2023, **10**, 4610–4631

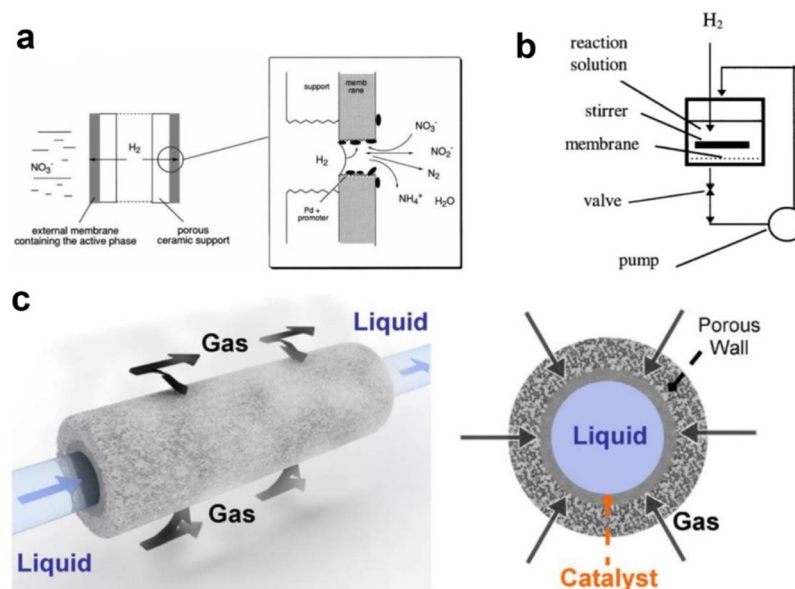This journal is © the Partner Organisations 2023

Fig. 2 (a) Schematic illustration of a catalytic membrane reactor for nitrate and nitrite reduction. (b) The flow-through configuration of a catalytic membrane reactor.[49] Copyright 2013, American Chemical Society. (c) The gas–liquid–solid contact in a porous ceramic reactor.[50] Copyright 2011, Elsevier.

Kinetically speaking, H*-rich conditions may provide selectivity for NH_3/NH_4^+, while nitrite-rich conditions favor N_2 formation, which is consistent with the conclusions from previous studies.[15,60] Detailed theoretical and experimental analyses regarding reaction selectivity will be discussed later in this review.

3. Activity

3.1. Thermal nitrite reduction by monometallic catalysts: activity

Due to the more favorable thermodynamics of the reaction pathways (Fig. 3, red pathways), the main product of thermal nitrate/nitrite reduction is usually N_2.[24,56,61,62] Previous studies have shown that many metal catalysts contribute to the catalytic initiation of nitrate (e.g., Cu, Sn, or In).[45,63–69] However, the subsequent reduction of nitrite and the production of subsequent intermediates depend mainly on the precious metal Pd. Seminal studies by Hörold et al.[70] and Soares et al.[71] tested the performance of Pt-group monometallics, including Pt, Ru, Ir, and Rh, but found low nitrite reduction activities. Besides, many properties of the catalysts (e.g., particle size, electronic structure, and the type of catalyst carrier) have been found to affect the nitrite reduction activity.

3.1.1 Particle size versus product activity. Catalysis is known to be site-specific.[73] The surface of metal NPs may consist of different types of catalytic sites, which can be qualitatively classified as high-coordination terraces and low-coordination edges and corners (Fig. 4).[72] Due to the significant difference in the adsorption properties, different sites exhibit different catalytic behaviors.[74–78] Besides, the proportion and

distribution of the sites are closely related to the size of metal particles. For this reason, the size of metal NPs can affect the catalytic activity of the catalyst. As shown in Fig. 5a, the Pd mass catalytic activities of the Pd catalysts with 2.1, 2.7, 4.0, 4.7, 5.6, 8.1, 18.2, and 22.1 nm were 508.5, 603.6, 442.1, 417.4, 348.6, 240.7, 131.3, and 111.8 mg g^{-1}_{Pd} min^{-1}, respectively. The catalytic activity decreased with the increase in the NP size. Notably, the mass activity of the 2.1 nm Pd catalyst was 508.5 mg g^{-1}_{Pd} min^{-1}, significantly lower than that of the 2.7 nm catalyst. This can be explained in conjunction with the TOF plot of Pd/C (Fig. 5b). The TOFs of the 2.1, 2.7, 4.0, 4.7, 5.6, 8.1, 18.2, and 22.1 nm Pd NPs were 462.9, 652.2, 710.3, 795.4, 839.5, 871.2, 996.1, and 1122.3 h^{-1}, respectively, indicating that the TOF increased significantly with the increase of the Pd NP size. Usually, a smaller NP size would lead to stronger adsorption strength to the adsorbates due to the lower average coordination number of the surface sites. Based on the Sabatier principle for heterogeneous catalysis, only a catalyst surface with moderate binding capacity can lead to optimal catalytic activity. Therefore, a plausible explanation for the observed trends in Fig. 5b is that those smaller-size Pd NPs generally overbind the reactants, leading to a lower TOF in nitrite reduction. In general, the catalyst mass activity depends on the total number of active sites and the intrinsic activity of each active site.[15,76,77] Therefore, the above results can be interpreted as follows: when the size of Pd NPs is larger than 2.7 nm, the decrease in the number of active sites plays a dominant role, leading to a decrease in macroscopic mass activity. When the size of Pd NPs is lower than 2.7 nm, the decrease of TOF plays a dominant role. In summary, when considering the relation between the particle size and catalytic activity, the TOF of the catalyst should be considered.
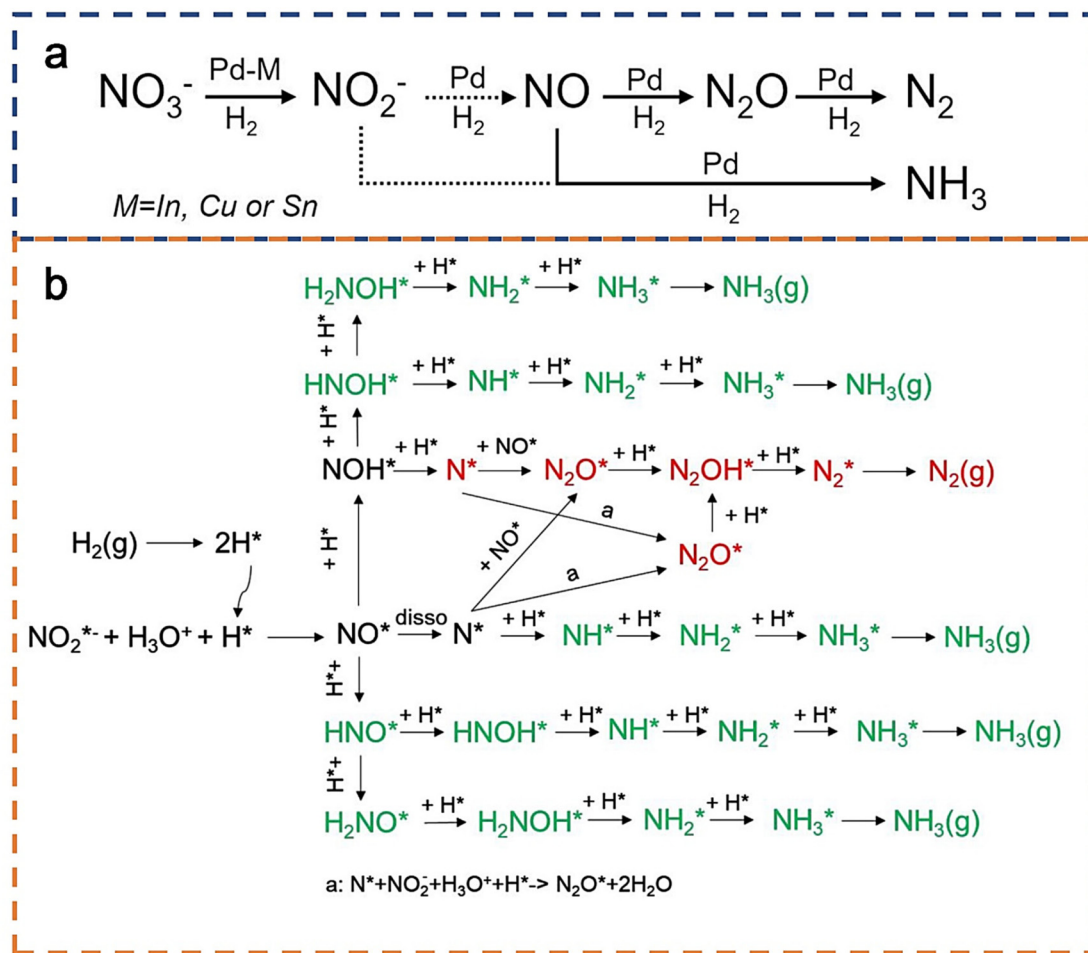
This journal is © the Partner Organisations 2023

Inorg. Chem. Front., 2023, **10**, 4610–4631 | **4613**

Fig. 3 (a) A general pathway for thermal nitrate reduction catalyzed by Pd-based catalysts with special element M as the promoter (M = In, Cu, or Sn).[29] Copyright 2017, American Chemical Society. (b) Reaction network of nitrite reduction using H_2 as the reducing agent. Red and green pathways represent the reaction selectivity towards N_2 and NH_3, respectively.[36] Copyright 2019, American Chemical Society. Note that after the formation of NH_3, NH_4^+ formation (not shown) is considered a facile process in the liquid-phase.
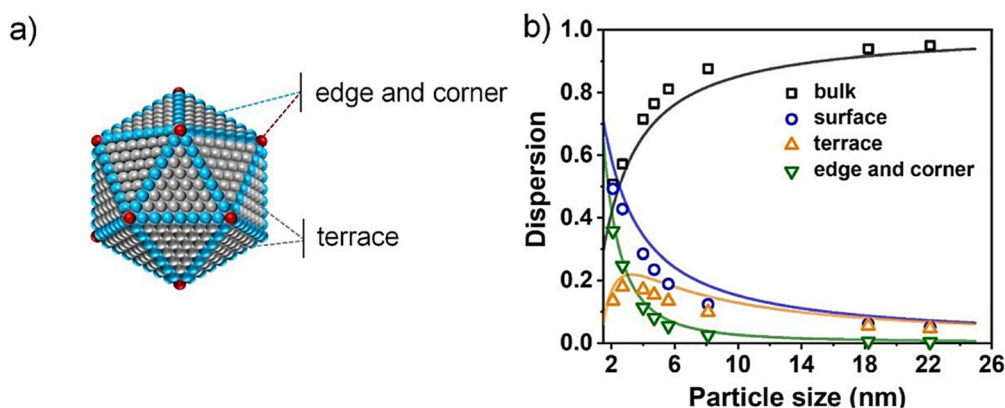

Fig. 4 (a) Schematic diagram of a structurally stable icosahedral Pd NP. (b) The ratio of bulk, surface, terrace, edge, and corner atoms on icosahedral Pd NPs with different sizes.[72] Copyright 2020, the Royal Society of Chemistry.

3.1.2 Electronic structure *versus* product activity. Another way to change the catalytic activity is to modulate the electronic structure of a catalyst. In numerous heterogeneous catalytic reactions,[80,81] adjusting the electronic structure of a catalyst can tune its catalytic activity.[79] This is because the electronic structure of a surface site plays an important role in reg-
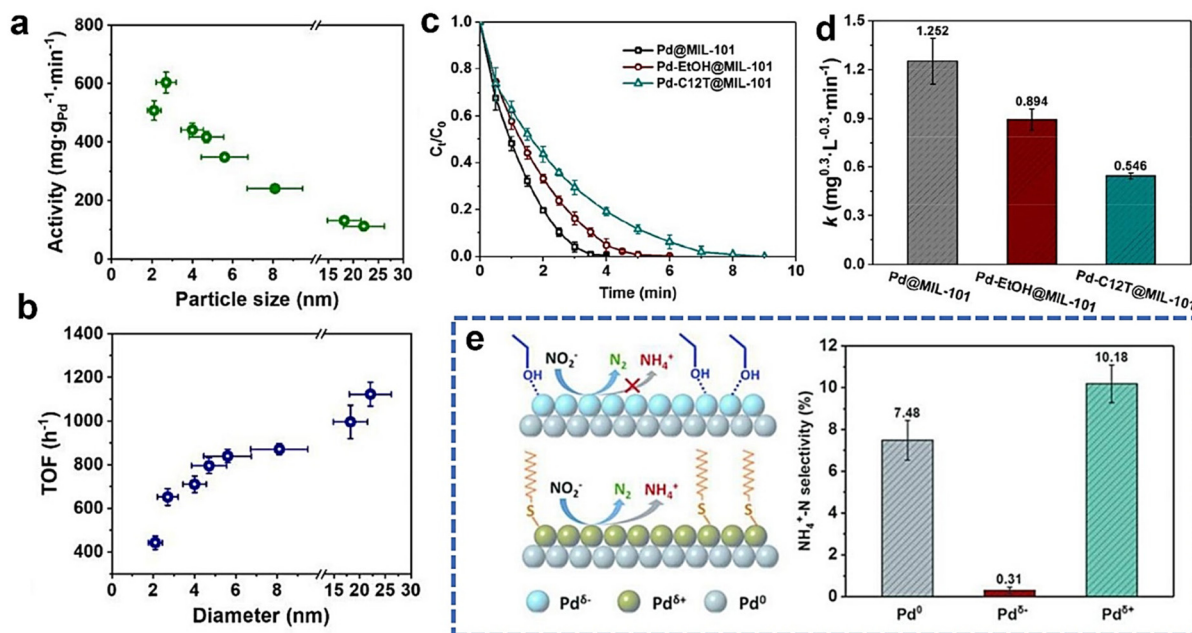
Fig. 5 (a and b) Nitrite reduction mass activity and TOF of Pd/C NPs with various sizes.[72] (c and d) Nitrite reduction performances of Pd catalysts with various treatment methods. Copyright 2020, the Royal Society of Chemistry. (e) Proposed relationships between the electronic structure of Pd catalysts and the experimentally measured nitrite reduction selectivity.[38] Copyright 2018, the Royal Society of Chemistry.

ulating the binding strengths of reactants and transition states. By adjusting the catalyst's electronic structure, the desired products may be obtained.[39,82] Fig. 5c–e shows the catalytic performance of three different catalysts for thermal nitrite reduction. It can be seen from Fig. 5c and d that the activity of the catalyst decreased after chelating ethanol and 1-dodecanethiol on the surface of Pd NPs. This could be attributed to the fact that the chelated ethanol and 1-dodecanethiol on the surface can reduce the number of Pd active sites and limit hydrogenation. It is noteworthy that the selectivity of ammonia is low when the Pd surface is electron-rich ($Pd^{\delta-}$), while the ammonia selectivity is high when its surface is electron-deficient ($Pd^{\delta+}$). Based on the explanations by Shin et al.[15] and Li et al.,[36] higher H-coverage under catalytic conditions would lead to higher ammonia selectivity in thermal nitrite reduction. Given that when a Pd surface is electron-deficient ($Pd^{\delta+}$), H-binding to the surface will be stronger, which would lead to higher H-coverage that promotes ammonia selectivity. In conclusion, adjusting the electronic states of the catalyst surface is effective in tuning the product selectivity, although there was a slight decrease in the catalytic activity (Fig. 5d).

3.2. Catalytic nitrate reduction by bimetallic catalysts: activity

During the past decades, great progress has been made in researching bimetallic alloy catalysts. It can be seen from Table 2 that many previous studies focused on developing alloy catalysts for thermal nitrate and nitrite reduction. The main reason for studying bimetallics is that when two metals are combined, the activity and selectivity are tuned by synergistic effects.[83] These effects can intrinsically be classified into

electronic (or ligand), strain, ensemble, and spin effects.[84,85] Seraj et al. showed that PdAu alloy NPs have higher catalytic reduction activities compared to pure Pd NPs.[29] Similar conclusions were obtained by Qian et al.[85] A series of bimetallic core@shell (Au@Pd) NPs were designed using a combination of experimental and computational approaches by Li et al.;[36] their catalyst design resulted in a high density of reactive Pd-sites on the surface of metal NPs, enhancing nitrite reduction activity.

The composition and structure of bimetallic alloys can also affect the catalyst's activity. Some previous research analyzed the effects of the catalyst composition and structure on nitrite reduction. For example, Qian et al. studied the catalytic structure–performance relationships of Pd NPs.[85] They used a two-step method to synthesize a catalyst with a special Pd-on-Au structure and found that the activity was related to the surface Pd coverage (Fig. 6e). Seraj et al.[29] found that Pd–Au alloy NPs have higher catalytic activities and resistance to sulfur-poisoning compared to pure Pd NPs. Li et al.[36] developed a combined experimental and theoretical strategy to find that the nitrite reduction performance of both monometallic and bimetallic catalysts can be evaluated by simple reaction descriptors, including the binding energies of N, N_2, and NH_3 at a surface site (Fig. 6a–c). They also found that bimetallic Pd-on-Au catalysts can optimize the surface activity of the active Pd sites and, meanwhile, maintain the maximum number of active Pd-sites on a surface. They found that a thin Pd layer [$Pd_{1monolayer}$/ Au (111)] deposited on Au NPs can lead to high nitrite reduction activity, with the experimental TOF superior to those of Pd and other Pd–Au alloys (Fig. 6f and g).

This journal is © the Partner Organisations 2023

Inorg. Chem. Front., 2023, **10**, 4610–4631 | **4615**

Table 2 Nitrate and nitrite reduction activity and selectivity of various catalysts, summarized from previous experimental reports

Materials	T (K)	Activity	S_{N_2} (%)	S_{NH_3} (%)	Ref.
PdAu	Room temp.	—	~100	—	36 [a]
Pd/TiO$_2$	Room temp.	—	90.9	9.1	15 [a]
Pd–PVA/Al$_2$O$_3$	294	1480 $\mu mol^{-1}\ L^{-1}\ g^{-1}\ min^{-1}$	—	—	86 [a]
Pd/Al$_2$O$_3$	294	1720 $\mu mol^{-1}\ L^{-1}\ g^{-1}\ min^{-1}$	—	—	86 [a]
Pd/γ-Al$_2$O$_3$	293	$1.7 \pm 0.4\ mmol\ g^{-1}\ min^{-1}$	—	—	86 [a]
Pd/C	298	$603.6\ mg\ g^{-1}_{Pd}\ min^{-1}$	93.2	6.8	72 [a]
Pd@MIL-101	298	$1.252\ mg^{0.3}\ L^{-0.3}\ min^{-1}$	18	82	38 [a]
Pd-ethanol@MIL-101	298	$0.894\ mg^{0.3}\ L^{-0.3}\ min^{-1}$	92.52	7.48	38 [a]
Pd-C12T@MIL-101	298	$0.546\ mg^{0.3}\ L^{-0.3}\ min^{-1}$	99.62	0.38	38 [a]
Rh/Al$_2$O$_3$	Room temp.	$\sim3\text{–}24\ L\ g^{-1}_{surface\ metal}\ min^{-1}$	~5–32	~68–95	87 [a]
AuNPs	295	Not active	—	—	29 [a]
Pd$_{53}$Au$_{47}$ NPs	295	$5.12\ L\ g^{-1}_{metal}\ min^{-1}$	—	<2	29 [a]
Pd NPs	295	$1.99\ L\ g^{-1}_{metal}\ min^{-1}$	—	<2	29 [a]
Pd$_{50}$Cu$_{50}$/PVP	Room temp.	$2.9\ L\ h^{-1}\ mmol^{-1}_{metal}$	96.8	3.2	60 [a]
Pd$_{70}$Cu$_{30}$/PVP	Room temp.	$4.2\ L\ h^{-1}\ mmol^{-1}_{metal}$	97	3	60 [a]
Pd/PVP	Room temp.	$0.3\ L\ h^{-1}\ mmol^{-1}_{metal}$	—	—	60 [a]
80sc% Pd-on-AuNPs	N/A	$576\ L\ g^{-1}_{Pd}\ min^{-1}$	99.6	0.4	85 [a]
Au@Pdmonolayer NPs	Room temp.	$246\ L\ g^{-1}_{surface\ Pd}\ min^{-1}$	97.5	2.5	36 [a]
Pd$_{95}$Ag$_5$NP–SiO$_2$	Room temp.	$4.61\ L\ g^{-1}_{Pd}\ min^{-1}$			34 [a]
PdNP–SiO$_2$	Room temp.	$1.35\ L\ g^{-1}_{Pd}\ min^{-1}$			34 [a]
Pd/Al$_2$O$_3$	~296	—	—	~100	87 [a]
Pd/CNFs	298	—	18	82	88 [a]
Cu$_x$Ir$_{1-x}$	Room temp.	—	—	~100	89 [a]
Pd–Cu/C	333	—	3.6	96.4	90 [a]
CNFs/Ni	Room temp.	—	~30	~70	91 [a]
40 sc% In-on-Pd NPs	Room temp.	$7.57 \pm 0.65\ L\ g^{-1}_{surface\ metal}\ min^{-1}$	—	—	55 [b]
Cu/NZVI	Room temp.	—	18	—	92 [b]
Cu–Pd/NZVI	Room temp.	$2.67\ mM\ NO_3^-$ per g_{cat} per h	60	—	93 [b]
Cu–Pd/TiO$_2$	Room temp.	—	50.2	47.7	94 [b]
Pd–Cu/TiO$_2$	293	$0.139\ g^{-1}_{cat}\ min^{-1}$	86.2	—	95 [b]
Sn–Pd-NZSM-5	Room temp.	$410 \times 10^{-2}\ L\ min^{-1}\ g^{-1}_{Pd}$	81	—	96 [b]
Cu–Pd-NBeta	Room temp.	—	92.68	—	97 [b]
Pd/Cu pillared clays	298	$68.9\ mmol\ min^{-1}\ g^{-1}_{Pd}$	—	25	98 [b]
Pd/Sn pillared clays	298	$82.7\ mmol\ min^{-1}\ g^{-1}_{Pd}$	—	16.5	98 [b]
Pd/In pillared clays	298	$57.4\ mmol\ min^{-1}\ g^{-1}_{Pd}$	—	12.2	98 [b]
Pd/Al particles	Room temp.	—	5.8	93.4	99 [b]
Ni/Al particles	Room temp.	—	—	99.6	99 [b]
Cu/Al particles	Room temp.	—	—	99.9	99 [b]
Sn–Pd/γ-Al$_2$O$_3$	Room temp.	$0.42\ mg\ L^{-1}\ g^{-1}\ min^{-1}$	70.1	—	100 [b]
Cu–Pd/AC	Room temp.	$2.017\ mmol\ h^{-1}\ g^{-1}_{cat}$	2.4	—	101 [b]
Cu–Pd/TiO$_2$	Room temp.	$0.356\ mmol\ h^{-1}\ g^{-1}_{cat}$	16.7	—	101 [b]
Cu–Pd/ZrO$_2$	Room temp.	$0.376\ mmol\ h^{-1}\ g^{-1}_{cat}$	8.9	—	101 [b]
Cu–Pd/Al$_2$O$_3$	Room temp.	$0.355\ mmol\ h^{-1}\ g^{-1}_{cat}$	0	—	101 [b]

[a] Nitrite reduction. [b] Nitrate reduction.

4. Selectivity

4.1. Catalytic nitrite reduction by monometallic catalysts: selectivity

In drinking water treatment, N_2 formation is desirable, while NH_3/NH_4^+ is more desirable for some emerging applications (e.g., ammonia production from waste treatment). Notably, N_2 or NH_3/NH_4^+ production is mainly at the active sites of some stronger-binding elements (e.g., Pd, Pt, and Rh).[18,20,36,38,102–105] Because of that, the selectivity of N_2 and NH_3/NH_4^+ production depends mainly on the reduction phase of nitrite on a strong-binding monometallic site.[24,106] Therefore, it is important to study the catalytic mechanism and factors that affect these metal sites and analyze the structure–selectivity relationships in nitrate and nitrite reduction.

4.1.1 Electronic structure *versus* product selectivity. Zhao et al.[107] studied the selectivity of nitrite reduction products by considering the electronic structure of the catalyst; they found that the ammonia formation selectivity was affected when the Pd surface was capped with polyvinylpyrrolidone (PVP) and was inhibited with the increase of PVP coverage. A plausible explanation is that PVP changed the electronic structure of the Pd surface. The relation between the electronic structure of Pd and the selectivity of nitrite reduction products was analyzed in depth by Zhang et al.,[38] showing that the selectivity of ammonia decreased when the electron density of Pd surface atoms increased (Pd$^{\delta-}$). This is because the change in the electronic structure of a Pd surface affects the activation energy of nitrite, which in turn affects the selectivity of ammonia formation (Fig. 7a). Meanwhile, the relationship between temperature and ammonia selectivity was analyzed; the selectivity
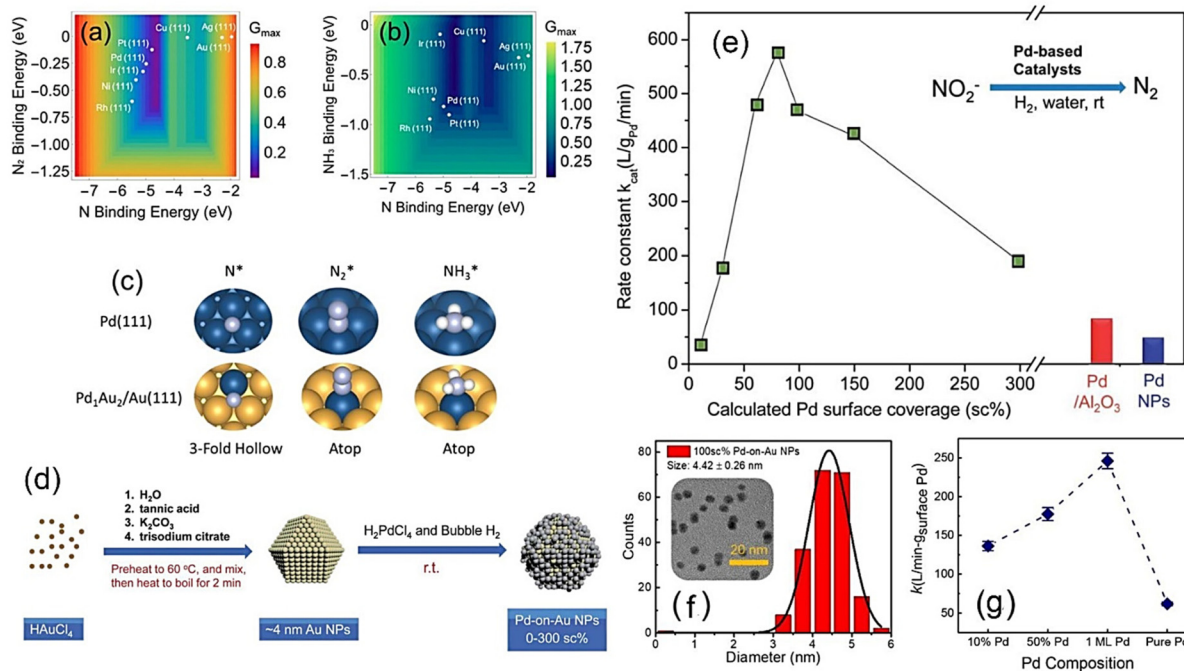
4616 | *Inorg. Chem. Front.*, 2023, **10**, 4610–4631

This journal is © the Partner Organisations 2023

Fig. 6 (a and b) Volcano-shaped predictive models for nitrite reduction through (a) N_2 and (b) NH_3/NH_4^+ formation pathways. (c) Typical optimized adsorption geometries on monometallic and bimetallic sites,[36] where the blue, yellow, light blue, and which spheres represent Pd, Au, N, and H atoms, respectively. (d) Two-stage synthesis of Pd-on-Au NPs considered for thermal nitrite reduction. Copyright 2019, American Chemical Society. (e) Experimentally determined nitrite reaction rate constants of various Pd-on-Au NPs.[85] Copyright 2014, Royal Society of Chemistry. (f) Particle size distributions of 100 sc% Pd-on-Au NPs. (g) Reaction kinetics of nitrite reduction on Pd-on-Au, Pd–Au alloys, and pure Pd NPs.[36] Copyright 2019, American Chemical Society.

of ammonia was found to increase with the increase of temperature, consistent with some previous studies.[43,70,108] This is mainly because ammonia production has a higher energy barrier ($\sim$48 kJ mol^{-1}) than N_2 formation.[108,109] In conclusion, the activation energy of nitrite can be changed by adjusting the electronic structure of Pd, which in turn can tune the product selectivity (Fig. 7b). Besides, increasing the reaction temperature can lead to a higher chance of ammonia production.

4.1.2 pH versus product selectivity. In addition to Pd, other noble metals (e.g., Rh, Ru, and Ir) generally have lower capacities for nitrite reduction and a lower selectivity for N_2 formation.[51,70] However, these conclusions are yet to be fully justified because they were measured based on the experimental conditions suitable for Pd. A slight change in the reaction conditions (e.g., pH) may lead to a significant change in product selectivity. Hörold et al. first proposed that pH is an important factor in nitrite hydrogenation,[70] where a lower pH favors the reduction of nitrite to N_2. However, in the absence of a buffer, the pH of the reaction solution increases as the reaction proceeds, thereby degrading the reaction performance. Clark et al.[87] studied the effects of pH on the reduction of nitrite to ammonia on a Rh surface (Fig. 7c and d); ammonia selectivity was up to 95% at pH = 11.5. They found that nitrite reduction on Rh was affected by NO* poisoning. However, this poisoning effect can be controlled by the solution pH. In other

words, at a low pH, the Rh surface was covered by NO*, which might poison the catalyst. Also, they found that the NO*/H* ratio on a Rh surface was regulated by the pH of the reaction medium, i.e., the dissociation of nitrite into NO* could be inhibited by adjusting the pH. For this reason, pH significantly influences the selectivity of NH_3/NH_4^+, and Rh favors the reduction of nitrite to NH_3/NH_4^+.[18,19,22,62] In conclusion, if the target product of nitrite reduction at higher pH reaction conditions is NH_3/NH_4^+, Pd may no longer be the best catalyst.

4.1.3 Particle size versus product selectivity. Section 3.1.1 discusses that the size of Pd NPs has a significant influence on the catalytic activity. Similarly, the product selectivity of thermal nitrite reduction can also be affected by particle size. It was found by theoretical and experimental studies that the selectivity of nitrite reduction on Pd is determined by the coverage of H* and N*.[15] Combined with the recent finding that an electron-deficient Pd surface leads to the selective formation of NH_3/NH_4^+,[38] it can be concluded that the selectivity of NH_3/NH_4^+ is dependent on the Pd structure. The characteristics and structural properties of Pd are closely related to the NP sizes. For this reason, researchers investigated the relationship between the Pd NP size and NH_3/NH_4^+ selectivity,[38] in which a too-large particle size is not favorable for ammonia formation. Moreover, the relationship between the particle size and activity may be related to the exposure of active sites. As shown in Fig. 8a, the number of exposed Pd sites increased
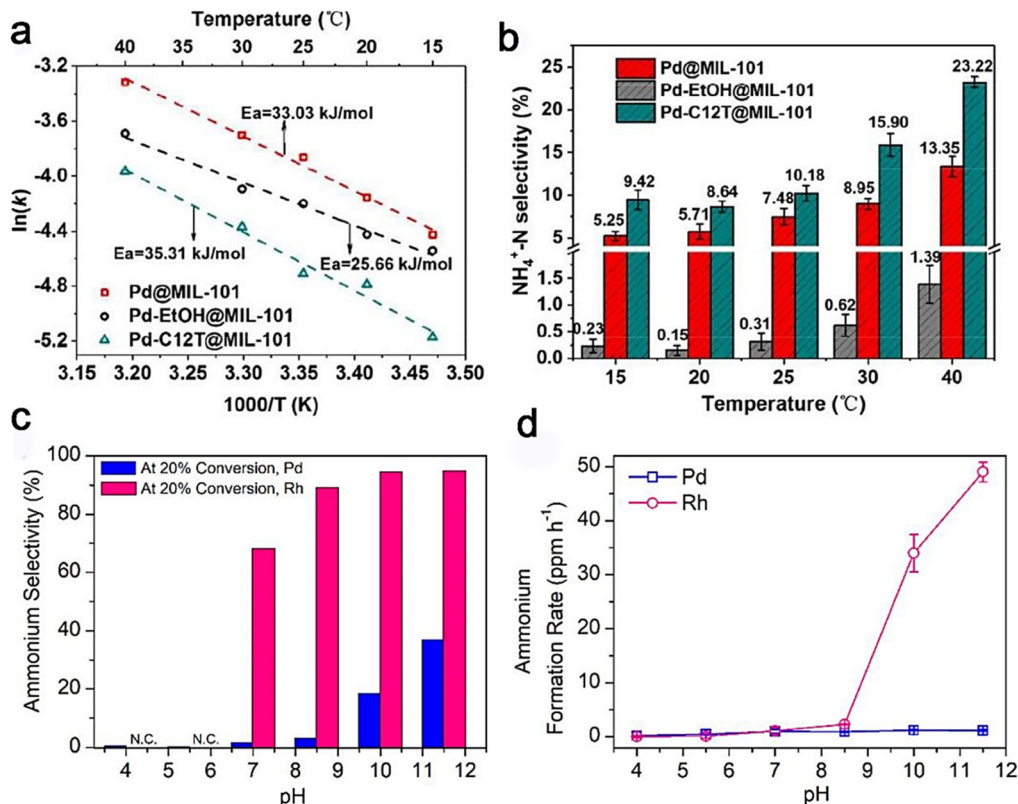
This journal is © the Partner Organisations 2023

Inorg. Chem. Front., 2023, **10**, 4610–4631 | **4617**

Fig. 7 (a) Experimental estimation of nitrite reduction activation energies (E_a) on different Pd surfaces. (b) Effects of the reaction temperature on ammonia selectivity on various Pd surfaces.[38] Copyright 2018, the Royal Society of Chemistry. (c and d) Effects of varying pH values on the selectivity of ammonia and the ammonia production rates on Pd and Rh.[87] Copyright 2019, American Chemical Society.

with the decrease of the Pd NP diameter, but the TOFs remained relatively stable with the increase of the Pd NP diameter (Fig. 8b). The change in the Pd NP size from 1.4 ± 0.7 to 9.6 ± 3.5 nm did not lead to a significant change in the TOF, and each exposed Pd site (e.g., edge, vertex, and plateau) had similar activities for nitrite reduction. The ammonia production percentages (NH_3%) versus nitrite reduction at different numbers/fractions of exposed Pd-sites and low-coordination Pd-sites are shown in Fig. 8c and d. Comparing all catalysts, the NH_3% value increases with the increased number of exposed Pd-sites and the increased proportion of low-coordination Pd sites, regardless of whether Pd is loaded inside or outside the CNF. This implies that NH_3% increases with the decrease of the Pd NP size. The main reason is that the number of exposed Pd sites or the fraction of low-coordination Pd sites increases monotonically with the decrease of the Pd NP size. The increase in ammonia production is due to the relatively small number of N–N pairings on the Pd NPs. A plausible reason is that N–N pairing becomes more difficult on smaller Pd islands with more low-coordination sites (i.e., edges and corners). Another possible reason is that N–N pairing is unfavorable on smaller Pd because the adsorbed N* has a lower chance of being adjacent to each other. The third possible reason is that nitrite reduction is faster on smaller Pd NPs, reducing the opportunity for N–N pairing.[35]

4.1.4 H_2 flow rate and NO_2^- concentration versus product selectivity. Previous studies also found that the reaction conditions (e.g., H_2 flow rate and NO_2^- concentration) had significant effects on the product selectivity of nitrite reduction. To illustrate the effects of the H_2 flow rate and NO_2^- concentration on the reaction, Shin et al.[15] used a combined theoretical and experimental strategy to study nitrite reduction on a Pd surface (Fig. 9). They found that the increase of H_2 flow can cause the enrichment of H* on Pd and the subsequent formation of ammonia. Due to this reason, increasing the flow rate of H_2 can facilitate NH_3/NH_4^+ formation. However, when increasing the concentration of NO_2^-, the N : H ratio increases, which in turn increases the chance of N–N pairing and thus favors N_2 production.

4.2. Catalyst design to improve activity and target-product selectivity

The rational design of a catalyst helps reduce the exhaustive experimental "trial-and-error" process in catalyst search. Based on the seminal Sabatier principle, a good heterogeneous catalyst should neither bond to the adsorbate too strongly nor too weakly.[110] Therefore, almost all the derived heterogeneous catalytic models present a "volcano-shape" as a function of the key adsorbate binding energies (i.e., adsorption energies) of the reaction.[111–123] A catalytic volcano model allows people to

4618 | Inorg. Chem. Front., 2023, 10, 4610–4631

This journal is © the Partner Organisations 2023

Fig. 8 (a) First-order rate constant (k) *versus* the number of exposed Pd sites. (b) TOFs *versus* Pd NP diameters. (c) Ammonia production percentage (NH$_3$%) *versus* the number of exposed Pd sites. (d) Ammonia production percentage (NH$_3$%) *versus* the fraction of low-coordination Pd sites.[35] Copyright 2021, American Chemical Society.

derive the optimal activity of catalysis. Therefore, catalyst design with the help of a volcano model can efficiently design promising catalysts with high activity and/or target-product selectivity.

4.2.1 Catalyst design for N$_2$ production

Model validation and active site identification. Before proceeding to design a new catalyst, the volcano activity plot should be determined beforehand. For thermal nitrite reduction, Li *et al.* derived the first volcano activity model for thermal nitrite reduction based on the linear scaling relations between the binding energies of N* and all other intermediate species.[36] The accuracy of the model was then evaluated by the benchmarking analyses with the experimental results of Seraj *et al.*[29] and Guy *et al.*[60] Fig. 10a and b shows the volcano activity model for nitrite reduction toward N$_2$ formation as a function of N* and N$_2$* binding energies, with the plotted binding energies calculated at various Pd–Au and Pd–Cu alloy (111) surfaces. It can be seen that only the 3-fold Pd$_3$ triatomic site on Pd$_{0.50}$Au$_{0.50}$(111) and Pd$_{0.75}$Cu$_{0.25}$(111) can reach the volcano peak, suggesting that ~50% and ~75% Pd on PdAu and PdCu, respectively, can lead to optimized nitrite reduction activity compared to other compositions. These are in excellent agreement with previous experiments that the optimal catalysts for nitrite reduction were ~53% and ~80% Pd, respectively, in Pd–Au and Pd–Cu nano-catalysts.[29,60] These benchmarking analyses clearly showed that this volcano model is precise and can

be used for predicting promising nitrite reduction catalysts as a function of nitrogen bonding strengths, which can significantly reduce computation costs. Interestingly, we can see that on Pd-based alloys, there is a synergy between the ligand and strain effects in tuning the N-binding energy at alloy surfaces. As shown in Fig. 10c and d, the N* binding energy at the close-packed Pd$_3$-site can reach the optimal region of the volcano due to the synergistic effects of the electronic change arising from the charge transfer between Pd and Au/Cu and the strain arising from the lattice difference between Pd and Au/Cu.

Optimizing and maximizing the most active sites: design of highly effective metal-on-metal catalysts. Volcano models can be used for the computational screening of promising catalysts. Those strongly bound metals are closer to the target binding energy than Au, Ag, and Cu. Also, X-on-Y (or core@shell-like) bimetallic structures can provide the maximum number of active sites on the catalytic surface, which can further increase the overall activity of a catalyst. For this purpose, Li *et al.*[36] modeled X-on-Y structures with X being a strong-binding metal (*e.g.*, Pd, Pt, Ir, Rh, and Ni) and Y being a typical weak-binding metal (*e.g.*, Au, Ag, and Cu) (Fig. 11). Fig. 11a–c shows that at least six of the screened catalysts are able to achieve the target activity (*i.e.*, theoretical optimal activity) indicated by the volcano model [Pd$_{3ML}$/Cu(111), Pd$_{2ML}$/Cu(111), Pd$_{1ML}$/Ag(111), Pt$_{3ML}$/Cu(111), Pd$_{1ML}$/Au(111), and Ni$_{1ML}$/Cu(111)]. Interestingly, most of these candidates are Pd-based catalysts,

This journal is © the Partner Organisations 2023

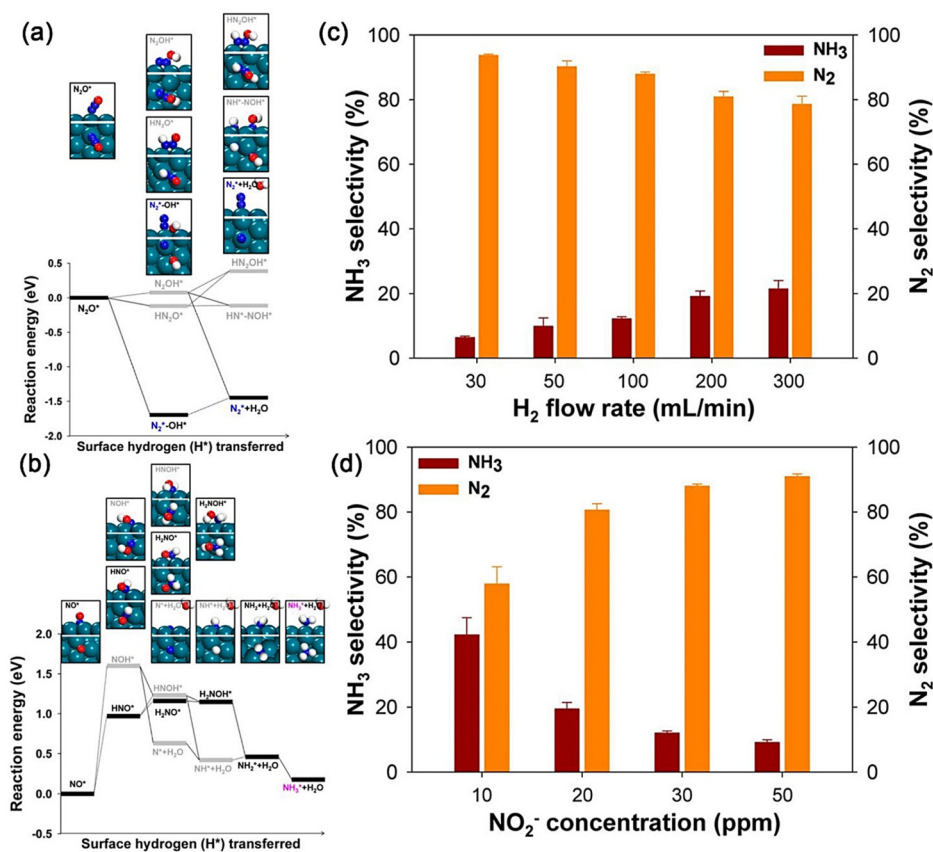*Inorg. Chem. Front.*, 2023, **10**, 4610–4631 | **4619**

Fig. 9 (a) Energy diagram of the hydrogenation pathway of NO* on a Pd(111) surface. (b) Energy diagram of the reduction of N_2O^* on Pd(111). Insets show the reaction intermediates considered for calculations. Green, blue, red, and white spheres represent Pd, N, O, and H atoms, respectively. (c and d) Experimentally measured N_2 and NH_3 selectivity of nitrite reduction at various (c) H_2 flow rates and (d) NO_2^- concentrations.[15] Copyright 2014, American Chemical Society.

suggesting that Pd is a promising element for nitrite reduction. Furthermore, most of these optimized catalysts have relatively weak N_2^* binding but strong NH_3^* binding, suggesting facile N_2 desorption and high selectivity for N_2 formation. To evaluate the stability of these candidates, their surface segregation energies were calculated (Fig. 11d). With N* adsorption, only the $Pd_{2ML}/Cu(111)$ and $Pd_{3ML}/Cu(111)$ surfaces have negative surface segregation energies. Therefore, it is expected that the remaining four catalysts could be stable in nitrite reduction under mild reaction conditions (*e.g.*, room temperature). Because Pd–Au can be synthesized by well-established methods, Pd-on-Au NPs were selected for experimental verification; the results showed that Pd-on-Au NPs had a relatively high selectivity (~100%) for N_2 formation compared to pure Pd NPs. In summary, the rational design of bimetallic catalysts based on the theoretical knowledge of alloying effects can help address complicated environmental problems.

4.2.2 Catalyst design for NH_3/NH_4^+ production. Most previous studies focused on the reduction of nitrite to N_2, while only a few have focused on the reduction of nitrite to NH_3/NH_4^+.[38,124] However, ammonia is an important precursor for agricultural and industrial chemicals. The Haber–Bosch method, which is currently the main process for ammonia syn-

thesis, is energy intensive and requires harsh reaction conditions (*e.g.*, T = 450 °C; P = 300 bar).[124] Therefore, catalytic reduction of nitrite for ammonia formation is a process that can create potential industrial values. Although the direct conversion of nitrate/nitrite into ammonia is not practical based on current technologies, a possible application scenario is that the ammonia-selective catalysts would be helpful to treat high nitrate/nitrite waste brine obtained from nitrate/nitrite removal technologies (*e.g.*, reverse osmosis and ion exchange) that are too expensive to discard. Li *et al.*[89] first found that due to the larger $5d_{z^2}$ orbitals at the 5d metal-atop site, these metals generally have larger H coverage under reaction conditions. This will lead to a kinetically more favorable NH_3 formation selectivity in nitrite reduction, as proven by Shin *et al.*[15] Based on these theoretical inspirations, they designed Ir and $Cu_xIr_{(100-x)}$ NPs for the reduction of nitrite to form NH_3/NH_4^+ by a combination of theoretical and experimental approaches. In their works, the main reasons for studying Ir-based alloys are as follows: (a) alloying cheap Cu with noble metal Ir reduces the dependence on expensive Ir; (b) in the volcano model of nitrite reduction toward ammonia formation (Fig. 12a), the straight line connecting Cu and Ir can go across the volcano peak, suggesting that a homogeneous Cu–Ir alloy
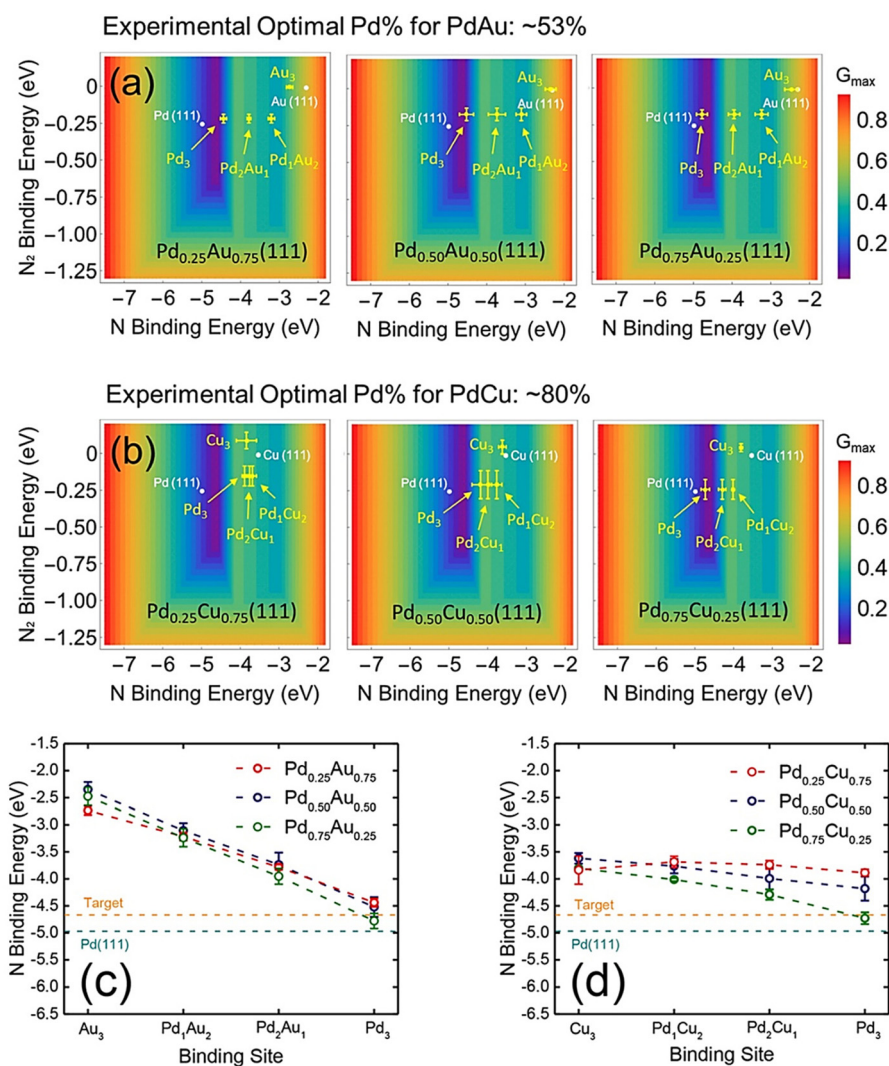
Fig. 10 (a and b) Predictions of thermal nitrite reduction at triatomic ensembles on PdAu and PdCu alloy surfaces. (c and d) N binding energies at the triatomic ensembles of PdAu and PdCu (111).[36] Copyright 2019, American Chemical Society.

(*i.e.*, solid-solution) could further tune the activity;[29,36,60,125] (c) alloying strong- and weak-binding metals could reduce adsorbate-poisoning;[29,82,126] and (d) there was very limited Ir-alloy catalysts that have been explored.[127,128] After synthesis, the powder X-ray diffraction (PXRD) patterns of the NPs confirmed the presence of solid-solution structures (Fig. 12d). Interestingly, the synthesized $Cu_xIr_{(100-x)}$ NPs showed nearly-100% NH_3/NH_4^+ formation selectivity (Fig. 12e). Instead of increasing the activity, alloying Cu into Ir led to a decrease in the activity, compared to pure Ir NPs (Fig. 12f). For example, the activity of pure Ir NPs was approximately ~5 times higher than that of $Cu_{49}Ir_{51}$ NPs. The main reason, as shown in Fig. 12g, is that significant electronic and strain effects are induced in Cu–Ir alloys,[83,126,129–131] making NH_3 tend to over-bind the Ir-atop site, which in turn breaks the linear scaling relation between N* and NH_3* bindings[132] and leads to a decrease in the activity of $Cu_xIr_{(100-x)}$ alloy NPs. Meanwhile, the H-coverage on the Ir-sites of Cu–Ir alloy is similar to that

of Ir(111), leading to superior NH_3/NH_4^+ selectivity (Fig. 12c). To generalize the findings of the experiments and enable further useful structure–function predictions, Li *et al.* screened other bimetallic surfaces mixed by 5d transition metals (Ir and Pt) and other metals (Fig. 12h), showing that alloying Pt with other inert transition metals (*e.g.*, Ag) will also ensure both high activity for nitrite reduction and ammonia formation selectivity.

5. Catalyst carrier *versus* activity and selectivity

To improve the dispersion of metals and to facilitate the separation and recovery of catalysts, Pd and other metals were often immobilized on support materials. Not only the properties of the metal particles but also the nature of the carrier and the strength of the metal–carrier interaction have significant
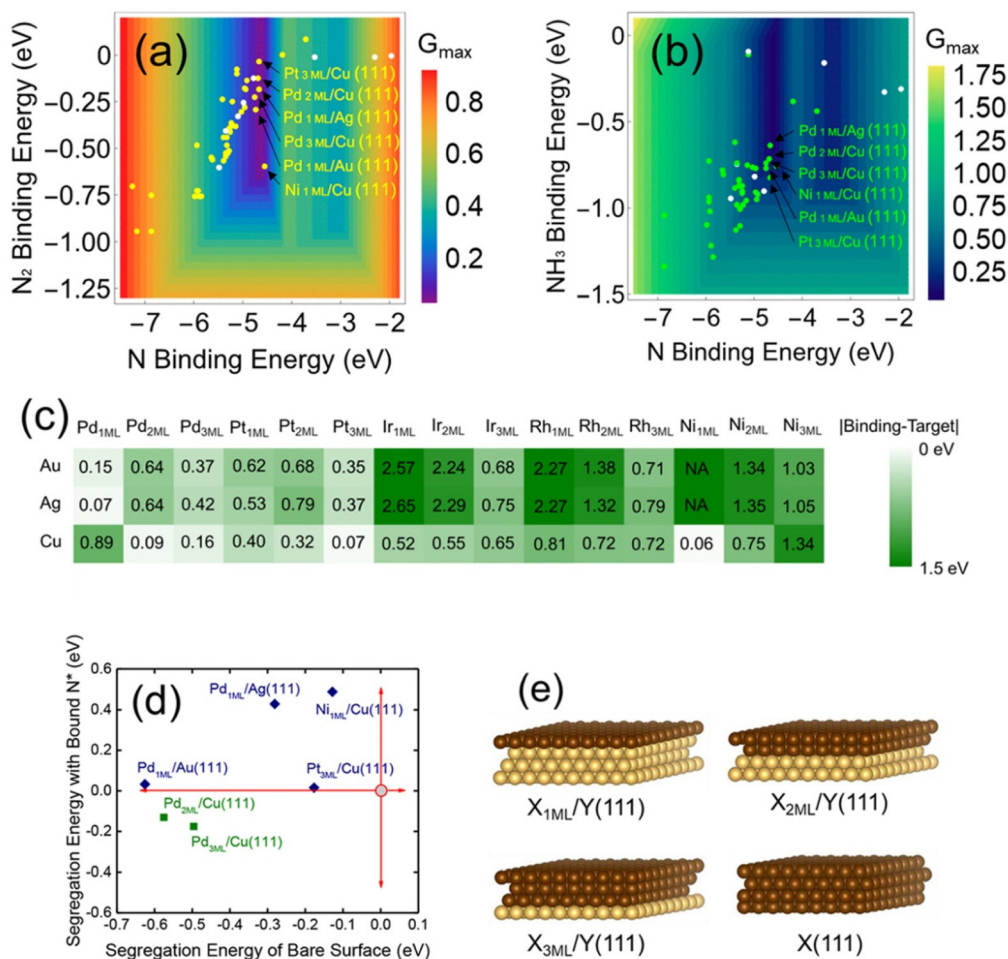
Fig. 11 (a and b) Volcano activity models with the plotted nitrogen bindings at X-on-Y (X = Pd, Pt, Rh, Ir, and Ni; Y = Au, Ag, and Cu) catalysts through the (a) N_2 and (b) NH_3 formation pathways illustrated in Fig. 4. (c) Matrix showing the surfaces with function quantified by |N binding-target binding|. (d) Calculated segregation energies with and without adsorbed N* on the X-on-Y catalysts. (e) Schematic pictures of X-on-Y models considered for theoretical calculations. Brown and gold spheres represent the X and Y elements, respectively.[36] Copyright 2019, American Chemical Society.

impacts on the catalyst performance. Reaction systems based on the thermal reduction of nitrite involve liquid–solid–gas triads. For this reason, the ideal surface properties of the catalyst are essential to ensure appropriate contact of the three phases and to eliminate internal and external diffusion limitations, thus achieving high activity and selectivity.

5.1.   Oxide carriers

Oxide carriers (e.g., γ-Al_2O_3, SiO_2, and TiO_2) were widely used as catalyst carriers due to their desirable properties (e.g., high surface area and porosity) and chemical stability. The abundant hydroxyl groups on the oxide surface can interact with the metal precursors and thus influence the position of the metal on the carrier.[133] This plays an important role in dispersing the active metal. According to previous studies,[20,134] γ-Al_2O_3 showed the highest catalytic activities with the highest nitrite reduction rates. It was found that the enhanced catalytic activity may be related to the small catalyst particle size produced on the γ-Al_2O_3 support. The void structure of the

support plays an important role in product selectivity. As studied by Krawczyk et al., SiO_2 with the smallest pore size of 1–5 nm showed the lowest N_2 selectivity (~56%), while TiO_2 with the largest pore size of 10–30 nm showed the highest N_2 selectivity (~88%).[135] This is related to the formation of an internal OH^- gradient in narrow pores:[136] OH^- formed in the narrow pore structure is difficult to neutralize because the diffusion of OH^- from the pore into the reaction medium is limited, resulting in the increase of local pH within the pore. As discussed in section 4.1.2, a higher pH promotes the formation of NH_3/NH_4^+. Therefore, small pore size supports tend to be more favorable for NH_3/NH_4^+ formation.[135,137]

5.2.   Carbon carriers

Carbon material carriers for nitrite reduction mainly include activated carbon (AC), carbon nanotubes (CNTs), and CNFs, among which AC is the most widely used because of its low cost and high availability. The high specific surface area and porosity allow the active metal to be fully dispersed on the
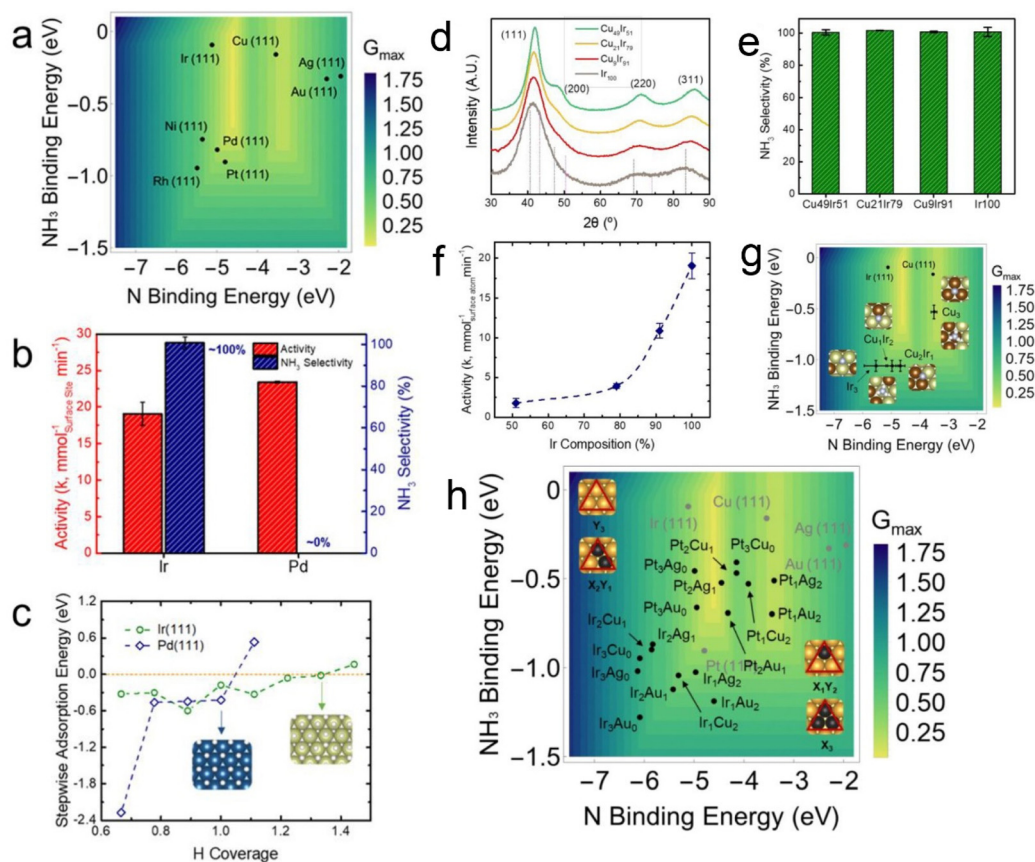
Fig. 12 (a) Volcano activity plot for nitrite reduction through the NH_3/NH_4^+ formation pathway. (b) Nitrite reduction activities and their ammonia selectivity on Pd and Ir NPs. (c) Stepwise adsorption energies of H* on Pd and Ir surfaces. (d) PXRD patterns of $Cu_xIr_{(100−x)}$ alloy NPs with different compositions. (e and f) Ammonia selectivity and the measured reaction rate constants of nitrite reduction on $Cu_xIr_{(100−x)}$ NPs. (g) Volcano activity model for nitrite reduction through the NH_3/NH_4^+ formation pathways with the data points of Ir, Cu, and the triatomic ensembles sampled from $Cu_{25}Ir_{75}$ surfaces. (h) Volcano activity model for nitrite reduction through the NH_3/NH_4^+ formation pathways with the triatomic ensembles at various alloy surfaces.[89] Copyright 2020, American Chemical Society.

carrier surface, resulting in smaller-size metal particles. These properties make carbon materials competitive candidates as carriers for Pd-based catalysts.[138] For AC carriers, due to the abundance of micropores, a rich void structure makes it easy to generate local pH gradients within the voids, favoring the production of NH_3/NH_4^+. According to previous studies, the selectivity of AC-supported PdCu catalysts for NH_3/NH_4^+ is often higher than 30%.[139,140] In addition, carbon materials are conductive, accelerating the electron transfer from the accessible Pd in the support shell to the less accessible Pd in the pores,[43] subsequently leading to an increase in H* concentration, which in turn is more favorable for NH_3/NH_4^+ production.

6. Thermal catalytic reduction *versus* electrocatalytic reduction

With the progress and development of detection technology and experimental technology, both thermal reduction and

electrocatalytic reduction are promising strategies for removing nitrate and/or nitrite.[27,141–151] A recent significant study compared the efficiency of these two methods for ammonia production *via* nitrate reduction (Fig. 13).[146] Fig. 13 (by Wang *et al.*[146]) illustrates that thermal nitrate reduction requires the availability of H_2, while electrocatalysis involves the participation of electrons and applied potentials.[11,21] Meanwhile, N_2 and NH_3/NH_4^+ are the main products for both methods. They analyzed the catalytic efficiency of the two methods in terms of the driving chemical potential, pH, nitrate concentration, and type of catalyst. Their experimental results, as summarized in Fig. 14, showed that increasing hydrogen pressure or electrochemical potential could promote nitrate conversion. It was also found that for alloy catalysts, the addition of Ru increased the adsorption strengths of nitrate and hydrogen as well as intermediate species, leading to higher catalytic activity. When the nitrate concentration was low, thermal and electrocatalytic nitrate reduction showed the same trend that a higher nitrate concentration can promote nitrite reduction. However, with a further increase in nitrate concentration (*i.e.*, >0.5 M), the rate
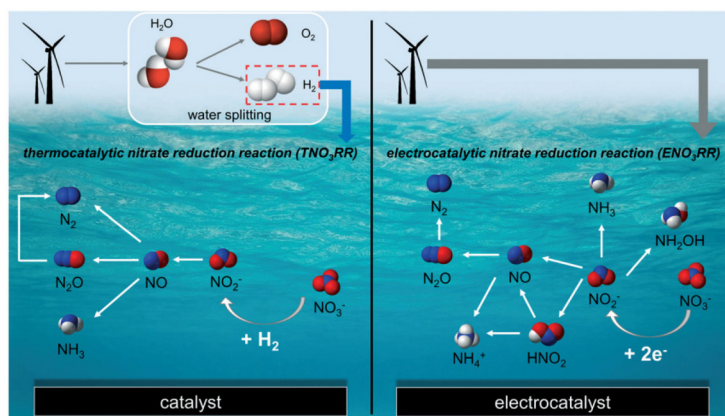
This journal is © the Partner Organisations 2023

Inorg. Chem. Front., 2023, **10**, 4610–4631 | **4623**

Fig. 13 Simplified reaction mechanism of the thermal nitrate reduction reaction (TNO$_3$RR) and the electrocatalytic nitrate reduction reaction (ENO$_3$RR).[146] Copyright 2018, the Royal Society of Chemistry.

of electrocatalytic nitrate reduction will decrease. This indicates that nitrate may block the surface sites for hydrogen adsorption and inhibit the reaction. The higher activity and lower E_a of thermal nitrite reduction at a lower pH are shown in Fig. 14c and d. These suggest that the higher nitrite hydrogenation TOF at a lower pH is mainly due to the increased surface coverage of reaction intermediates such as *NO and *HNO.[147] When pH = 1, the reaction had a lower E_a value, possibly due to the more favorable conversion of intermediates to ammonia at a low pH value. The effects of pH on electrocatalytic nitrate reduction are shown in Fig. 14c and d. Wang et al.[146] suggested that pH affects the charge on the electrode surface, which in turn can tune the catalytic activity. The essential part of the work by Wang et al.[146] is the feasibility comparison between the two reduction methods. An ideal catalytic system must be of low cost and must exhibit higher ammonia production efficiency as shown in Fig. 14f. For thermal nitrate reduction (reaction conditions: PtRu/C; pH = 1), the ammonia production rate was high, and the process cost was in line with the economic requirements. This shows that thermal nitrate reduction is expected to be a potential alternative to the Haber–Bosch method under milder conditions.

Interestingly, there is a difference in the proposed mechanisms for thermal and electrocatalytic nitrate reduction. For electrocatalytic nitrate reduction, the reduction of nitrate to nitrite could be a rate-determining step on many catalysts,[152] while for thermal nitrate reduction, this step is considered non-rate-limiting on some typical catalysts (e.g., In–Pd catalysts).[54] Regarding why thermal nitrate reduction to nitrite on some In-based catalysts is not rate-limiting, one possibility is that the surface states (e.g., adsorbate coverage) of a catalyst under electrocatalytic conditions and thermal hydrogenation could be very different,[153] leading to different energetics in the first step of nitrate reduction. However, to the best of our knowledge, almost no previous study has paid attention to this difference in the reaction mechanism between thermal and electrocatalytic nitrate reduction, and thus it is still an interest-

ing open question in the nitrate conversion process. Note that one of the most obvious differences in designing thermal and electrocatalytic nitrate/nitrite reduction catalysts is that their surface states (i.e., adsorbate coverage) under reaction conditions could be very different. For example, in thermal nitrate/nitrite reduction, hydrogen will be activated and will precover on the surface; therefore, the adsorbate coverage will depend on the reaction temperature, nitrate/nitrite concentration, and H$_2$ pressure. While in room-temperature electrocatalytic nitrate/nitrite reduction, due to the equilibrium between water and the adsorbates after potential-induced water activation (e.g., H*, HO*, and O*),[153] the adsorbate coverage will depend on the applied potential, nitrate/nitrite concentration, and pH.[154] These intrinsic differences in the surface states would lead to very different reaction environments that make the reaction energetics different. Therefore, when designing thermal and electrocatalytic nitrate/nitrite reduction catalysts, the surface phase diagrams should be analyzed before analyzing the reaction activity.

7. Challenges in the thermal catalytic reduction of nitrate and nitrite

Despite the great potential and opportunities of thermal nitrate and nitrite reduction in water treatment, some key obstacles may hamper its large-scale applications, which are summarized as follows.

(1) Most of the catalysts reported to date are based on precious metals, which are associated with high costs in catalyst preparation. This also hampers the potential commercialization of this nitrate/nitrite removal method. Many of the lower-cost materials that can potentially be stable under reaction conditions, such as less-noble metals and some metal X-ides (TMX, where X = O, N, C, B, F, Cl, Br, etc.), are much less explored. This may be because the research population to study thermal nitrate/nitrite reduction is relatively small (Fig. 1).
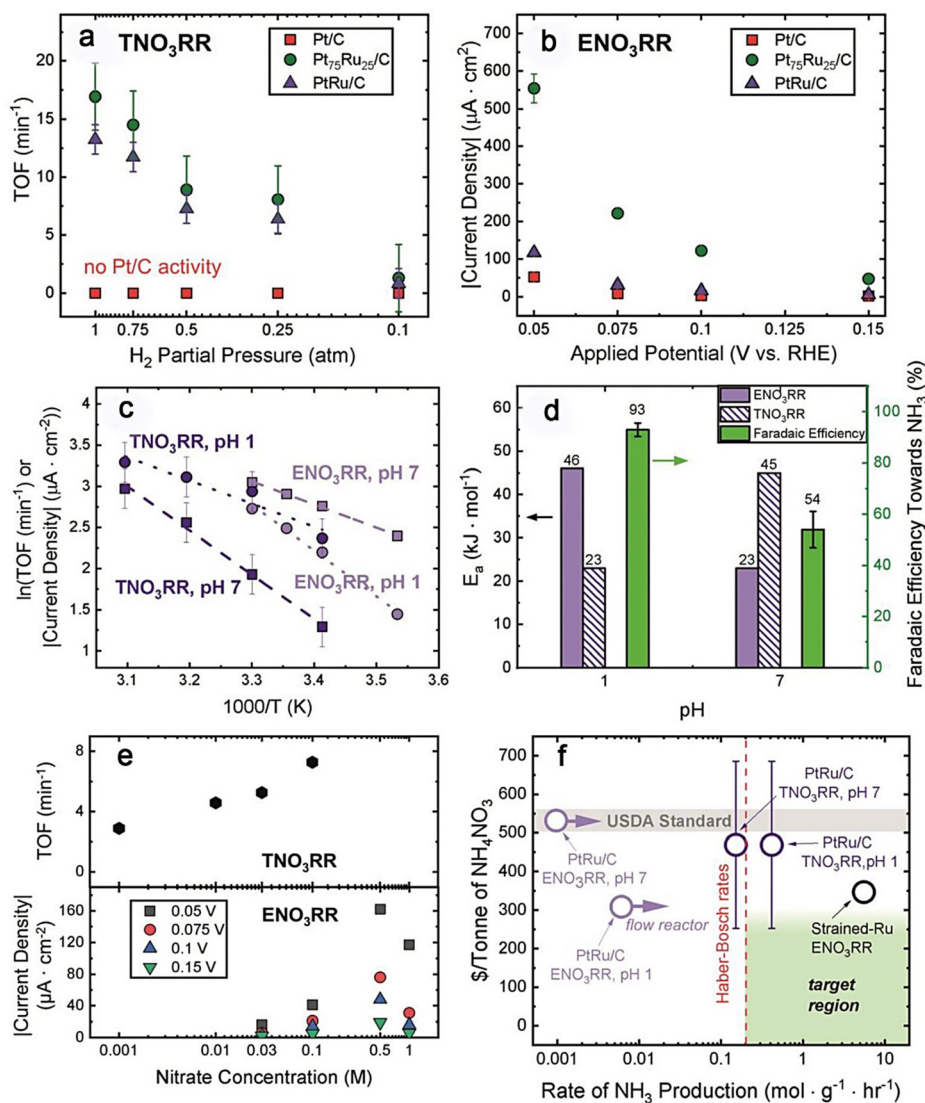
4624 | Inorg. Chem. Front., 2023, 10, 4610–4631

This journal is © the Partner Organisations 2023

Fig. 14 (a) TOFs of thermal catalytic nitrate reduction *versus* hydrogen partial pressures on different Pt-based catalysts. (b) Current densities of electrocatalytic nitrate reduction *versus* the applied potentials on different Pt-based catalysts. (c) Arrhenius plots of nitrate reduction on PtRu/C. (d) Comparison of apparent activation energy (E_a) *versus* faradaic efficiency (FE) towards NH_3/NH_4^+ across different solution pH values and systems. (e) The activity of PtRu/C as a function of nitrate concentration at pH = 7. (f) Comparison of the economic value of two different methods.[146] Copyright 2021, the Royal Society of Chemistry.

(2) The harsh conditions in wastewater bodies impose stricter requirements on thermal nitrate and nitrite reduction catalysts, including high thermal and chemical stability. However, long-term stability evaluation of the related catalysts reported so far was generally dismissed. After long-term operating conditions for nitrate/nitrite reduction, active-site poisoning/blocking or adsorbate-induced surface segregation could occur, which may in turn lead to catalyst deactivation.

(3) There is no uniform standard so far to fairly evaluate the activity of a thermal nitrate and nitrite reduction catalyst. For example, how to confirm the nitrogen source of the formed N_2 and NH_3/NH_4^+? Perhaps, isotope labeling experiments, which have been proven essential for electrocatalytic ammonia synthesis,

could also be necessary for detecting the products in thermal nitrate/nitrite reduction.

(4) It is difficult to find a catalyst with high activity and target-product selectivity, especially catalysts targeting ammonia formation. So far, the catalyst search strategy for thermal nitrate/nitrite reduction still mainly relies on a trial-and-error process from experiments. Better catalyst design strategies, such as theory-orientated catalyst design,[89] should receive more attention.

8. Perspectives and conclusion

Although thermal nitrate and nitrite reduction is still not as "popular" as the electrochemical reduction of nitrate/nitrite, it

This journal is © the Partner Organisations 2023

Inorg. Chem. Front., 2023, **10**, 4610–4631 | **4625**

is expected to be an active research area in the future given that it is important in wastewater treatment and its significant potential to form value-added ammonia upon rational catalyst design. The tremendous development of green hydrogen production and safe hydrogen transportation techniques endow the thermal reduction of nitrate and nitrite with a new future. Because this reaction is much less explored compared to electrocatalytic reduction, some fundamental and engineering questions need to be further explored, including:

(1) Why some promoters (*e.g.*, Cu, Sn, and In) can reduce nitrate to nitrite but cannot effectively reduce nitrite?

(2) Are there any effective and target-product selective catalysts beyond precious metals?

(3) Can we use other safer sources (*e.g.*, hydrogen storage materials) to provide H* in water treatment instead of molecular hydrogen?

To address these key questions, *in situ*/*operando* methods and more comprehensive theoretical models need to be developed. For example, surface phase diagrams need to be developed to fully understand the state of the Cu, Sn, or In promoter on a Pd-based catalyst surface in a reaction environment, while *in situ* surface probing methods would be helpful in understanding the surface state of the catalyst. With solid answers to the above questions, the key challenges of nitrate and nitrite reduction can be addressed by developing a more rational design strategy for a catalyst, accompanied by new engineering methods for wastewater treatment.

Conflicts of interest

There are no conflicts to declare.

Acknowledgements

References

1 A. Liu, J. Ming and R. O. Ankumah, Nitrate contamination in private wells in rural Alabama, United States, *Sci. Total Environ.*, 2005, **346**, 112–120.

2 B. T. Nolan and J. D. Stoner, Nutrients in groundwaters of the conterminous United States, 1992–1995, *Environ. Sci. Technol.*, 2000, **34**, 1156–1165.

3 L. Fewtrell, Drinking-water nitrate, methemoglobinemia, and global burden of disease: a discussion, *Environ. Health Perspect.*, 2004, **112**, 1371–1374.

4 S. Guo, C. D. Powell, D. Villagrán and M. S. Wong, Magnetic In-Pd catalysts for nitrate degradation, *Environ. Sci.: Nano*, 2020, **7**, 2681–2690.

5 A. R. Townsend, R. W. Howarth, F. A. Bazzaz, M. S. Booth, C. C. Cleveland, S. K. Collinge and A. H. Wolfe, Human health effects of a changing global nitrogen cycle, *Front. Ecol. Environ.*, 2003, **1**, 240–246.

6 R. L. Seiler, Combined use of ^{15}N and ^{18}O of nitrate and ^{11}B to evaluate nitrate contamination in groundwater, *Appl. Geochem.*, 2005, **20**, 1626–1636.

7 P. J. Weyer, J. R. Cerhan and B. C. Kross, Municipal drinking water nitrate level and cancer risk in older women: the Iowa Women's Health Study, *Epidemiology*, 2001, 327–338.

8 C. P. Ahada and S. Suthar, Groundwater nitrate contamination and associated human health risk assessment in southern districts of Punjab, India, *Environ. Sci. Pollut. Res.*, 2018, **25**, 25336–25347.

9 S. M. A. Adelana, Nitrate health effects, *Water encyclopedia*, 2005, **4**, 30–42.

10 US.EPA, *National Primary Drinking Water Regulations and Contaminant Candidate List*, US.EPA, 2008.

11 EU, Council Directive 98/83/EC, Official Journal of the European Communities, Brussel, 1998.

12 WHO, *Guidelines for drinking-water quality*, World Health Organization, 3rd edn, 2006.

13 L. Mattarozzi, S. Cattarin, N. Comisso, P. Guerriero, M. Musiani, L. Vázquez-Gómez and E. Verlato, Electrochemical reduction of nitrate and nitrite in alkaline media at CuNi alloy electrodes, *Electrochim. Acta*, 2013, **89**, 488–496.

14 E. Filloux, J. Wang, M. Pidou, W. Gernjak and Z. Yuan, Biofouling and scaling control of reverse osmosis membrane using one-step cleaning-potential of acidified nitrite solution as an agent, *J. Membr. Sci.*, 2015, **495**, 276–283.

15 H. Shin, S. Jung, S. Bae, W. Lee and H. Kim, Nitrite reduction mechanism on a Pd surface, *Environ. Sci. Technol.*, 2014, **48**, 12768–12774.

16 J. Chung, R. Nerenberg and B. E. Rittmann, Evaluation for biological reduction of nitrate and perchlorate in brine water using the hydrogen-based membrane biofilm reactor, *J. Environ. Eng.*, 2007, **133**, 157–164.

17 G. Centi and S. Perathoner, Remediation of water contamination using catalytic technologies, *Appl. Catal., B*, 2003, **41**, 15–29.

18 J. Martínez, A. Ortiz and I. Ortiz, State-of-the-art and perspectives of the catalytic and electrocatalytic reduction of aqueous nitrates, *Appl. Catal., B*, 2017, **207**, 42–59.

19 W. Teng, N. Bai, Y. Liu, J. Fan and W. X. Zhang, Selective nitrate reduction to dinitrogen by electrocatalysis on nanoscale iron encapsulated in mesoporous carbon, *Environ. Sci. Technol.*, 2018, **52**, 230–236.

20 K. D. Vorlop and T. Tacke, Erste schritte auf dem weg zur edelmetallkatalysierten nitrat-und nitrit-entfernung aus trinkwasser, *Chem. Ing. Tech.*, 1989, **61**, 836–837.

21 F. Epron, F. Gauthard, C. Pinéda and J. Barbier, Catalytic reduction of nitrate and nitrite on Pt-Cu/Al$_2$O$_3$ catalysts in aqueous solution: role of the interaction between copper and platinum in the reaction, *J. Catal.*, 2001, **198**, 309–318.

22 A. Pintar, J. Batista, J. Levec and T. Kajiuchi, Kinetics of the catalytic liquid-phase hydrogenation of aqueous nitrate solutions, *Appl. Catal., B*, 1996, **11**, 81–98.

23 I. Balint, A. Miyazaki and K. I. Aika, NO reduction by CH$_4$ over well-structured Pt nanocrystals supported on γ-Al$_2$O$_3$, *Appl. Catal., B*, 2002, **37**, 217–229.

24 U. Prüsse and K. D. Vorlop, Supported bimetallic palladium catalysts for water-phase nitrate reduction, *J. Mol. Catal. A: Chem.*, 2001, **173**, 313–328.

25 J. Wang, T. Feng, J. Chen, V. Ramalingam, Z. Li, D. M. Kabtamu and X. Fang, Electrocatalytic nitrate/nitrite reduction to ammonia synthesis using metal nanocatalysts and bio-inspired metalloenzymes, *Nano Energy*, 2021, **86**, 106088.

26 N. M. Deraz, The comparative jurisprudence of catalysts preparation methods: I. Precipitation and impregnation methods, *J. Ind. Environ. Chem.*, 2018, **2**, 19–21.

27 J. Aluha, K. Bere, N. Abatzoglou and F. Gitzhofer, Synthesis of nano-catalysts by induction suspension plasma technology (SPS) for Fischer-Tropsch reaction, *Plasma Chem. Plasma Process.*, 2016, **36**, 1325–1348.

28 J. Taghavimoghaddam, G. P. Knowles and A. L. Chaffee, Preparation and characterization of mesoporous silica supported cobalt oxide as a catalyst for the oxidation of cyclohexanol, *J. Mol. Catal. A: Chem.*, 2012, **358**, 79–88.

29 S. Seraj, P. Kunal, H. Li, G. Henkelman, S. M. Humphrey and C. J. Werth, PdAu alloy nanoparticle catalysts: effective candidates for nitrite reduction in water, *ACS Catal.*, 2017, **7**, 3268–3276.

30 K. G. N. Quiton, M. C. Lu and Y. H. Huang, Synthesis and catalytic utilization of bimetallic systems for wastewater remediation: A review, *Chemosphere*, 2021, **262**, 128371.

31 A. Devard, M. A. Ulla and F. A. Marchesini, Synthesis of Pd/Al$_2$O$_3$ coating onto a cordierite monolith and its application to nitrite reduction in water, *Catal. Commun.*, 2013, **34**, 26–29.

32 P. Xu, S. Agarwal and L. Lefferts, Mechanism of nitrite hydrogenation over Pd/γ-Al$_2$O$_3$ according a rigorous kinetic study, *J. Catal.*, 2020, **383**, 124–134.

33 A. F. Lee, P. J. Ellis, I. J. Fairlamb and K. Wilson, Surface catalysed Suzuki-Miyaura cross-coupling by Pd nanoparticles: an operando XAS study, *Dalton Trans.*, 2010, **39**, 10473–10482.

34 J. P. Troutman, H. Li, A. M. Haddix, B. A. Kienzle, G. Henkelman, S. M. Humphrey and C. J. Werth, PdAg alloy nanocatalysts: toward economically viable nitrite reduction in drinking water, *ACS Catal.*, 2020, **10**, 7979–7989.

35 D. Shuai, J. K. Choe, J. R. Shapley and C. J. Werth, Enhanced activity and selectivity of carbon nanofiber supported Pd catalysts for nitrite reduction, *Environ. Sci. Technol.*, 2021, **46**, 2847–2855.

36 H. Li, S. Guo, K. Shin, M. S. Wong and G. Henkelman, Design of a Pd-Au nitrite reduction catalyst by identifying and optimizing active ensembles, *ACS Catal.*, 2019, **9**, 7957–7966.

37 J. Lee, Y. G. Hur, M. S. Kim and K. Y. Lee, Catalytic reduction of nitrite in water over ceria-and ceria-zirconia-supported Pd catalysts, *J. Mol. Catal. A: Chem.*, 2015, **399**, 48–52.

38 Z. Zhang, W. Shi, W. Wang, Y. Xu, X. Bao, R. Zhang and F. Cui, Interfacial electronic effects of palladium nanocatalysts on the by-product ammonia selectivity during nitrite catalytic reduction, *Environ. Sci.: Nano*, 2018, **5**, 338–349.

39 A. Miyazaki, T. Asakawa, Y. Nakano and I. Balint, Nitrite reduction on morphologically controlled Pt nanoparticles, *Chem. Commun.*, 2005, **29**, 3730–3732.

40 J. P. Troncéa, S. V. I. Parvulescu and P. Granger, Unexpected kinetic behavior of structured Pd/CeO$_2$-ZrO$_2$ toward undesired ammonia formation and consumption during nitrites reduction: role of the reactivity of oxygen from ceria, *Catal. Today*, 2022, **383**, 330–338.

41 S. D. Ebbesen, B. L. Mojet and L. Lefferts, In situ ATR-IR study of nitrite hydrogenation over Pd/Al$_2$O$_3$, *J. Catal.*, 2021, **256**, 15–23.

42 J. K. Chinthaginjala, A. Villa, D. S. Su, B. L. Mojet and L. Lefferts, Nitrite reduction over Pd supported CNFs: Metal particle size effect on selectivity, *Catal. Today*, 2012, **183**, 119–123.

43 J. K. Chinthaginjala and L. Lefferts, Support effect on selectivity of nitrite reduction in water, *Appl. Catal., B*, 2010, **101**, 144–149.

44 B. P. Chaplin, J. R. Shapley and C. J. Werth, The selectivity and sustainability of a Pd-In/γ-Al$_2$O$_3$ catalyst in a packed-bed reactor: the effect of solution composition, *Catal. Lett.*, 2009, **130**, 56–62.

45 Y. X. Chen, Y. Zhang and H. Y. Liu, Reduction of nitrate from groundwater: powder catalysts and catalytic membrane, *J. Environ. Sci.*, 2003, **15**, 600–606.

46 Y. X. Chen, Y. Zhang, H. Y. Liu, K. R. Sharma and G. H. Chen, Hydrogen-based tubular catalytic membrane for removing nitrate from groundwater, *Environ. Technol.*, 2004, **25**, 227–234.

47 K. Daub, G. Emig, M. J. Chollier, M. Callant and R. Dittmeyer, Studies on the use of catalytic membranes for reduction of nitrate in drinking water, *Chem. Eng. Sci.*, 1999, **54**, 1577–1582.

48 N. Wehbe, N. Guilhaume, K. Fiaty, S. Miachon and J. A. Dalmon, Hydrogenation of nitrates in water using mesoporous membranes operated in a flow-through catalytic contactor, *Catal. Today*, 2010, **156**, 208–215.

49 H. C. Aran, J. K. Chinthaginjala, R. Groote, T. Roelofs, L. Lefferts, M. Wessling and R. G. Lammertink, Porous ceramic mesoreactors: a new approach for gas-liquid con-

This journal is © the Partner Organisations 2023

Inorg. Chem. Front., 2023, **10**, 4610–4631 | **4627**

tacting in multiphase microreaction technology, *Chem. Eng. J.*, 2011, **169**(1–3), 239–246.

50 N. Diban, A. T. Aguayo, J. Bilbao, A. Urtiaga and I. Ortiz, Membrane reactors for in situ water removal: a review of applications, *Ind. Eng. Chem. Res.*, 2013, **52**, 10342–10354.

51 S. Hörold, K. D. Vorlop, T. Tacke and M. Sell, Development of catalysts for a selective nitrate and nitrite removal from drinking water, *Catal. Today*, 1993, **17**, 21–30.

52 B. P. Chaplin, M. Reinhard, W. F. Schneider, C. Schüth, J. R. Shapley, T. J. Strathmann and C. J. Werth, Critical review of Pd-based catalytic treatment of priority contaminants in water, *Environ. Sci. Technol.*, 2012, **46**, 3655–3670.

53 H. L. Tierney, A. E. Baber, J. R. Kitchin and E. C. H. Sykes, Hydrogen dissociation and spillover on individual isolated palladium atoms, *Phys. Rev. Lett.*, 2009, **103**, 246102.

54 S. Guo, H. Li, K. N. Heck, X. Luan, W. Guo, G. Henkelman and M. S. Wong, Gold boosts nitrate reduction and de-activation resistance to indium-promoted palladium catalysts, *Appl. Catal., B*, 2022, **305**, 121048.

55 S. Guo, K. Heck, S. Kasiraju, H. Qian, Z. Zhao, L. C. Grabow and M. S. Wong, Insights into nitrate reduction over indium-decorated palladium nanoparticle catalysts, *ACS Catal.*, 2018, **8**, 503–515.

56 U. Prüsse, M. Hähnlein, J. Daum and K. D. Vorlop, Improving the catalytic nitrate reduction, *Catal. Today*, 2000, **55**, 79–90.

57 J. Sá and J. A. Anderson, FTIR study of aqueous nitrate reduction over Pd/TiO$_2$, *Appl. Catal., B*, 2008, **77**, 409–417.

58 R. Zhang, D. Shuai, K. A. Guy, J. R. Shapley, T. J. Strathmann and C. J. Werth, Elucidation of nitrate reduction mechanisms on a Pd-In bimetallic catalyst using isotope labeled nitrogen species, *ChemCatChem*, 2013, **5**, 313–321.

59 S. Jung, S. Bae and W. Lee, Development of Pd-Cu/hematite catalyst for selective nitrate reduction, *Environ. Sci. Technol.*, 2014, **48**, 9651–9658.

60 K. A. Guy, H. Xu, J. C. Yang, C. J. Werth and J. R. Shapley, Catalytic nitrate and nitrite reduction with Pd-Cu/PVP colloids in water: Composition, structure, and reactivity correlations, *J. Phys. Chem. C*, 2009, **113**, 8177–8185.

61 B. P. Chaplin, E. Roundy, K. A. Guy, J. R. Shapley and C. J. Werth, Effects of natural water ions and humic acid on catalytic nitrate reduction kinetics using an alumina supported Pd-Cu catalyst, *Environ. Sci. Technol.*, 2006, **40**, 3075–3081.

62 V. Urbain, R. Benoit and J. Manem, Membrane bioreactor: a new treatment tool, *J. - Am. Water Works Assoc.*, 1996, **88**, 75–86.

63 Y. B. Yin, S. Guo, K. N. Heck, C. A. Clark, C. L. Conrad and M. S. Wong, Treating water by degrading oxyanions using metallic nanostructures, *ACS Sustainable Chem. Eng.*, 2018, **6**, 11160–11175.

64 X. Zhu, X. C. Zeng, X. Chen, W. Wu and Y. Wang, Inhibitory effect of nitrate/nitrite on the microbial reduc-tive dissolution of arsenic and iron from soils into pore water, *Ecotoxicology*, 2019, **28**, 528–538.

65 B. P. Chaplin, J. R. Shapley and C. J. Werth, Regeneration of sulfur-fouled bimetallic Pd-based catalysts, *Environ. Sci. Technol.*, 2007, **41**, 5491–5497.

66 F. A. Marchesini, S. Irusta, C. Querini and E. Miró, Nitrate hydrogenation over Pt, In/Al$_2$O$_3$ and Pt, In/SiO$_2$. Effect of aqueous media and catalyst surface properties upon the catalytic activity, *Catal. Commun.*, 2008, **9**, 1021–1026.

67 F. A. Marchesini, S. Irusta, C. Querini and E. Miró, Spectroscopic and catalytic characterization of Pd-In and Pt-In supported on Al$_2$O$_3$ and SiO$_2$, active catalysts for nitrate hydrogenation, *Appl. Catal., A*, 2008, **348**, 60–70.

68 A. Pintar, J. Batista and I. Muševič, Palladium-copper and palladium-tin catalysts in the liquid phase nitrate hydrogenation in a batch-recycle reactor, *Appl. Catal., B*, 2004, **52**, 49–60.

69 Y. Xie, H. Cao, Y. Li, Y. Zhang and J. C. Crittenden, Highly selective PdCu/amorphous silica-alumina (ASA) catalysts for groundwater denitration, *Environ. Sci. Technol.*, 2011, **45**, 4066–4072.

70 S. Hörold, T. Tacke and K. D. Vorlop, Catalytical removal of nitrate and nitrite from drinking water: 1. Screening for hydrogenation catalysts and influence of reaction conditions on activity and selectivity, *Environ. Technol.*, 1993, **14**, 931–939.

71 O. S. G. Soares, J. J. Órfão and M. F. R. Pereira, Activated carbon supported metal catalysts for nitrate and nitrite reduction in water, *Catal. Lett.*, 2008, **126**, 253–260.

72 Z. Zhang, J. Lu, B. Zhang, W. Shi, Y. Guo and F. Cui, Insight into the size effect of Pd nanoparticles on the catalytic reduction of nitrite in water over Pd/C catalysts, *Environ. Sci.: Nano*, 2020, **7**, 2117–2129.

73 J. K. Nørskov, T. Bligaard, B. Hvolbæk, F. Abild-Pedersen, I. Chorkendorff and C. H. Christensen, The nature of the active site in heterogeneous metal catalysis, *Chem. Soc. Rev.*, 2008, **37**, 2163–2171.

74 D. Gao, H. Zhou, J. Wang, S. Miao, F. Yang, G. Wang and X. Bao, Size-dependent electrocatalytic reduction of CO$_2$ over Pd nanoparticles, *J. Am. Chem. Soc.*, 2015, **137**, 4288–4291.

75 S. H. Joo, J. Y. Park, J. R. Renzas, D. R. Butcher, W. Huang and G. A. Somorjai, Size effect of ruthenium nanoparticles in catalytic carbon monoxide oxidation, *Nano Lett.*, 2010, **10**, 2709–2713.

76 H. U. I. Zhang, M. Jin, Y. Xiong, B. Lim and Y. Xia, Shape-controlled synthesis of Pd nanocrystals and their catalytic applications, *Acc. Chem. Res.*, 2013, **46**, 1783–1794.

77 X. F. Yang, A. Wang, B. Qiao, J. Li, J. Liu and T. Zhang, Single-atom catalysts: a new frontier in heterogeneous catalysis, *Acc. Chem. Res.*, 2013, **46**, 1740–1748.

78 J. Y. Park, Y. Zhang, S. H. Joo, Y. Jung and G. A. Somorjai, Size effect of RhPt bimetallic nanoparticles in catalytic activity of CO oxidation: Role of surface segregation, *Catal. Today*, 2012, **181**, 133–137.

4628 | *Inorg. Chem. Front.*, 2023, **10**, 4610–4631

This journal is © the Partner Organisations 2023

79 G. Chen, C. Xu, X. Huang, J. Ye, L. Gu, G. Li and N. Zheng, Interfacial electronic effects control the reaction selectivity of platinum catalysts, *Nat. Mater.*, 2016, **15**, 564–569.

80 K. Gong, F. Du, Z. Xia, M. Durstock and L. Dai, Nitrogen-doped carbon nanotube arrays with high electrocatalytic activity for oxygen reduction, *science*, 2009, **323**, 760–764.

81 H. Zhang, T. Watanabe, M. Okumura, M. Haruta and N. Toshima, Catalytically highly active top gold atom on palladium nanocluster, *Nat. Mater.*, 2012, **11**, 49–52.

82 L. Jin, B. Liu, S. S. Duay and J. He, Engineering surface ligands of noble metal nanocatalysts in tuning the product selectivity, *Catalysts*, 2017, **7**, 44.

83 H. Li, K. Shin and G. Henkelman, Effects of ensembles, ligand, and strain on adsorbate binding to alloy surfaces, *J. Chem. Phys.*, 2018, **149**(17), 174705.

84 A. Cao, V. J. Bukas, V. Shadravan, Z. Wang, H. Li, J. Kibsgaard and J. K. Nørskov, A spin promotion effect in catalytic ammonia synthesis, *Nat. Commun.*, 2022, **13**, 1–7.

85 H. Qian, Z. Zhao, J. C. Velazquez, L. A. Pretzer, K. N. Heck and M. S. Wong, Supporting palladium metal on gold nanoparticles improves its catalysis for nitrite reduction, *Nanoscale*, 2014, **6**, 358–364.

86 Y. Zhao, N. K. Rao and L. Lefferts, Adsorbed species on Pd catalyst during nitrite hydrogenation approaching complete conversion, *J. Catal.*, 2016, **337**, 102–110.

87 C. A. Clark, C. P. Reddy, H. Xu, K. N. Heck, G. Luo, T. P. Senftle and M. S. Wong, Mechanistic insights into pH-controlled nitrite reduction to ammonia and hydrazine over rhodium, *ACS Catal.*, 2019, **10**, 494–509.

88 Y. Yoshinaga, T. Akita, I. Mikami and T. Okuhara, Hydrogenation of nitrate in water to nitrogen over Pd-Cu supported on active carbon, *J. Catal.*, 2002, **207**, 37–45.

89 H. Li, C. Yan, H. Guo, K. Shin, S. M. Humphrey, C. J. Werth and G. Henkelman, $Cu_x Ir_{1-x}$ Nanoalloy Catalysts Achieve Near 100% Selectivity for Aqueous Nitrite Reduction to NH_3, *ACS Catal.*, 2020, **10**, 7915–7921.

90 I. Mikami, Y. Sakamoto, Y. Yoshinaga and T. Okuhara, Kinetic and adsorption studies on the hydrogenation of nitrate and nitrite in water using Pd-Cu on active carbon support, *Appl. Catal., B*, 2003, **44**, 79–86.

91 R. Brunet Espinosa and L. Lefferts, Ni in CNFs: highly active for nitrite hydrogenation, *ACS Catal.*, 2016, **6**, 5432–5440.

92 S. Bae, S. Hamid, J. Jung, Y. Sihn and W. Lee, Effect of promoter and noble metals and suspension pH on catalytic nitrate reduction by bimetallic nanoscale Fe^0 catalysts, *Environ. Technol.*, 2016, **37**, 1077–1087.

93 S. Hamid, S. Bae, W. Lee, M. T. Amin and A. A. Alazba, Catalytic nitrate removal in continuous bimetallic Cu-Pd/nanoscale zerovalent iron system, *Ind. Eng. Chem. Res.*, 2015, **54**, 6247–6257.

94 S. Bae, J. Jung and W. Lee, The effect of pH and zwitterionic buffers on catalytic nitrate reduction by TiO_2-supported bimetallic catalyst, *Chem. Eng. J.*, 2013, **232**, 327–337.

95 Q. Wang, W. Wang, B. Yan, W. Shi, F. Cui and C. Wang, Well-dispersed Pd-Cu bimetals in TiO_2 nanofiber matrix with enhanced activity and selectivity for nitrate catalytic reduction, *Chem. Eng. J.*, 2017, **326**, 182–191.

96 S. Hamid, M. A. Kumar and W. Lee, Highly reactive and selective Sn-Pd bimetallic catalyst supported by nanocrystalline ZSM-5 for aqueous nitrate reduction, *Appl. Catal., B*, 2016, **187**, 37–46.

97 S. Hamid, M. A. Kumar, J. I. Han, H. Kim and W. Lee, Nitrate reduction on the surface of bimetallic catalysts supported by nano-crystalline beta-zeolite (NBeta), *Green Chem.*, 2017, **19**, 853–866.

98 A. H. Pizarro, C. B. Molina, J. J. Rodriguez and F. Epron, Catalytic reduction of nitrate and nitrite with mono-and bimetallic catalysts supported on pillared clays, *J. Environ. Chem. Eng.*, 2015, **3**(4), 2777–2785.

99 W. Zhao, X. Zhu, Y. Wang, Z. Ai and D. Zhao, Catalytic reduction of aqueous nitrates by metal supported catalysts on Al particles, *Chem. Eng. J.*, 2014, **254**, 410–417.

100 S. Hao and H. Zhang, High catalytic performance of nitrate reduction by synergistic effect of zero-valent iron (Fe^0) and bimetallic composite carrier catalyst, *J. Cleaner Prod.*, 2017, **167**, 192–200.

101 Y. Sakamoto, Y. Kamiya and T. Okuhara, Selective hydrogenation of nitrate to nitrite in water over Cu-Pd bimetallic clusters supported on active carbon, *J. Mol. Catal. A: Chem.*, 2016, **250**(1–2), 80–86.

102 R. Gavagnin, L. Biasetto, F. Pinna and G. Strukul, Nitrate removal in drinking waters: the effect of tin oxides in the catalytic hydrogenation of nitrate by Pd/SnO_2 catalysts, *Appl. Catal., B*, 2002, **38**, 91–99.

103 O. S. G. Soares, J. J. Orfao and M. F. R. Pereira, Pd-Cu and Pt-Cu catalysts supported on carbon nanotubes for nitrate reduction in water, *Ind. Eng. Chem. Res.*, 2010, **49**, 7183–7192.

104 P. Granger, S. Troncéa, J. P. Dacquin, M. Trentesaux and V. I. Parvulescu, Support-induced effect on the catalytic properties of Pd particles in water denitrification: Impact of surface and structural features of mesoporous ceria-zirconia support, *Appl. Catal., B*, 2018, **224**, 648–659.

105 A. S. Sekhar, A. Zaki, S. Troncea, S. Casale, C. P. Vinod, J. P. Dacquin and P. Granger, Enhanced selectivity of 3-D ordered macroporous Pt/Al_2O_3 catalysts in nitrites removal from water, *Appl. Catal., A*, 2018, **564**, 26–32.

106 C. A. Boasiako, Z. Zhou, X. Huo and T. Ye, Development of Pd-based Catalysts for Hydrogenation of Nitrite and Nitrate in Water: A Review, *J. Hazard. Mater.*, 2002, 130661.

107 Y. Zhao, J. A. Baeza, N. K. Rao, L. Calvo, M. A. Gilarranz, Y. D. Li and L. Lefferts, Unsupported PVA-and PVP-stabilized Pd nanoparticles as catalyst for nitrite hydrogenation in aqueous phase, *J. Catal.*, 2014, **318**, 162–169.

108 T. Tacke and K. D. Vorlop, Kinetische charakterisierung von katalysatoren zur selektiven entfernung von nitrat und nitrit aus wasser, *Chem. Ing. Tech.*, 1993, **65**, 1500–1502.

This journal is © the Partner Organisations 2023

Inorg. Chem. Front., 2023, **10**, 4610–4631 | 4629

109 S. K. Ghosh, S. Nath, S. Kundu, K. Esumi and T. Pal, Solvent and ligand effects on the localized surface plasmon resonance (LSPR) of gold colloids, *J. Phys. Chem. B*, 2004, **108**, 13963–13971.

110 A. J. Medford, A. Vojvodic, J. S. Hummelshøj, J. Voss, F. Abild-Pedersen, F. Studt and J. K. Nørskov, From the Sabatier principle to a predictive theory of transition-metal heterogeneous catalysis, *J. Catal.*, 2015, **328**, 36–42.

111 H. Li, S. Kelly, D. Guevarra, Z. Wang, Y. Wang, J. A. Haber and J. K. Nørskov, Analysis of the limitations in the oxygen reduction activity of transition metal oxide surfaces, *Nat. Catal.*, 2021, **4**, 463–468.

112 M. Stamatakis, Kinetic modelling of heterogeneous catalytic systems, *J. Phys.: Condens. Matter*, 2014, **27**, 013001.

113 A. Cao, Z. Wang, H. Li and J. K. Nørskov, Relations between surface oxygen vacancies and activity of methanol formation from CO_2 hydrogenation over In_2O_3 surfaces, *ACS Catal.*, 2021, **11**, 1780–1786.

114 H. Li, S. Xu, M. Wang, Z. Chen, F. Ji, K. Cheng and W. Yang, Computational design of (100) alloy surfaces for the hydrogen evolution reaction, *J. Mater. Chem. A*, 2020, **8**, 17987–17997.

115 G. W. Piburn, H. Li, P. Kunal, G. Henkelman and S. M. Humphrey, Rapid Synthesis of Rhodium-Palladium Alloy Nanocatalysts, *ChemCatChem*, 2018, **10**, 329–333.

116 H. Li, A. Cao and J. K. Nørskov, Understanding Trends in Ethylene Epoxidation on Group IB Metals, *ACS Catal.*, 2021, **11**, 12052–12057.

117 L. Zhou, H. Li, Y. Lai, M. Richter, K. Kan, J. A. Haber and J. M. Gregoire, Stability and Activity of Cobalt Antimonate for Oxygen Reduction in Strong Acid, *ACS Energy Lett.*, 2022, **7**, 993–1000.

118 S. Pan, H. Li, D. Liu, R. Huang, X. Pan, D. Ren and X. Zhang, Efficient and stable noble-metal-free catalyst for acidic water oxidation, *Nat. Commun.*, 2022, **13**, 1–10.

119 W. Yang, X. Chen, Y. Feng, F. Wang, Z. Gao, Y. Liu and H. Li, Understanding trends in the mercury oxidation activity of single-atom catalysts, *Environ. Sci.: Nano*, 2022, **9**, 2041–2050.

120 H. Li, C. S. Abraham, M. Anand, A. Cao and J. K. Nørskov, Opportunities and Challenges in Electrolytic Propylene Epoxidation, *J. Phys. Chem. Lett.*, 2022, **13**, 2057–2063.

121 Y. Liu, C. Xu, W. Cen and H. Li, Design strategy of bifunctional catalysts for CO oxidation, *Fuel*, 2022, **320**, 123909.

122 W. Yang, Y. Feng, X. Chen, C. Wu, F. Wang, Z. Gao and H. Li, Understanding Trends in the NO Oxidation Activity of Single-Atom Catalysts, *J. Environ. Chem. Eng.*, 2022, **10**, 108744.

123 W. Yang, B. Zhou, Z. Jia, C. Wu, L. Wei, Z. Gao and H. Li, Coordination Engineering of Single-Atom Iron Catalysts for Oxygen Evolution Reaction, *ChemCatChem*, 2022, **14**, e202201016.

124 J. W. Erisman, M. A. Sutton, J. Galloway, Z. Klimont and W. Winiwarter, How a century of ammonia synthesis changed the world, *Nat. Geosci.*, 2008, **1**, 636–639.

125 S. García, L. Zhang, G. W. Piburn, G. Henkelman and S. M. Humphrey, Microwave synthesis of classically immiscible rhodium-silver and rhodium-gold alloy nanoparticles: Highly active hydrogenation catalysts, *ACS Nano*, 2014, **8**, 11512–11521.

126 H. Li, W. Chai and G. Henkelman, Selectivity for ethanol partial oxidation: the unique chemistry of single-atom alloy catalysts on Au, Ag, and Cu (111), *J. Mater. Chem. A*, 2019, **7**, 23868–23877.

127 H. Guo, H. Li, K. Jarvis, H. Wan, P. Kunal, S. G. Dunning and S. M. Humphrey, Microwave-assisted synthesis of classically immiscible Ag-Ir alloy nanoparticle catalysts, *ACS Catal.*, 2018, **8**, 11386–11397.

128 H. Guo, Z. Fang, H. Li, D. Fernandez, G. Henkelman, S. M. Humphrey and G. Yu, Rational design of rhodium-iridium alloy nanoparticles as highly active catalysts for acidic oxygen evolution, *ACS Nano*, 2019, **13**, 13225–13234.

129 G. Xiao, R. Lu, J. Liu, X. Liao, Z. Wang and Y. Zhao, Coordination environments tune the activity of oxygen catalysis on single atom catalysts: A computational study, *Nano Res.*, 2022, **15**, 3073–3081.

130 M. Mavrikakis, B. Hammer and J. K. Nørskov, Effect of strain on the reactivity of metal surfaces, *Phys. Rev. Lett.*, 1998, **81**, 2819.

131 P. Liu and J. K. Nørskov, Ligand and ensemble effects in adsorption on alloy surfaces, *Phys. Chem. Chem. Phys.*, 2001, **3**, 3814–3818.

132 E. M. Fernández, P. G. Moses, A. Toftelund, H. A. Hansen, J. I. Martínez, F. Abild-Pedersen and J. K. Nørskov, Scaling relationships for adsorption energies on transition metal oxide, sulfide, and nitride surfaces, *Angew. Chem., Int. Ed.*, 2008, **47**, 4683–4686.

133 J. A. Schwarz, C. Contescu and A. Contescu, Methods for preparation of catalytic materials, *Chem. Rev.*, 1995, **95**, 477–510.

134 B. A. Mehrabadi, S. Eskandari, U. Khan, R. D. White and J. R. Regalbuto, A review of preparation methods for supported metal catalysts, *Adv. Catal.*, 2017, **61**, 1–35.

135 N. Krawczyk, S. Karski and I. Witońska, The effect of support porosity on the selectivity of Pd-In/support catalysts in nitrate reduction, *React. Kinet., Mech. Catal.*, 2011, **103**, 311–323.

136 M. D'Arino, F. Pinna and G. Strukul, Nitrate and nitrite hydrogenation with Pd and Pt/SnO_2 catalysts: the effect of the support porosity and the role of carbon dioxide in the control of selectivity, *Appl. Catal., B*, 2004, **53**, 161–168.

137 A. H. Pizarro, I. Torija and V. M. Monsalvo, Enhancement of Pd-based catalysts for the removal of nitrite and nitrate from water, *J. Water Supply: Res. Technol.–AQUA*, 2018, **67**, 615–625.

138 F. Rodriguez-Reinoso, The role of carbon materials in heterogeneous catalysis, *Carbon*, 1998, **36**, 159–175.

139 L. Calvo, M. A. Gilarranz, J. A. Casas, A. F. Mohedano and J. J. Rodriguez, Denitrification of water with activated carbon-supported metallic catalysts, *Ind. Eng. Chem. Res.*, 2020, **49**, 5603–5609.

4630 | *Inorg. Chem. Front.*, 2023, **10**, 4610–4631

This journal is © the Partner Organisations 2023

140 J. Trawczyński, P. Gheek, J. Okal, M. Zawadzki and M. I. Gomez, Reduction of nitrate on active carbon supported Pd-Cu catalysts, *Appl. Catal., A*, 2011, **409**, 39–47.

141 O. S. G. Soares, J. J. Órfão and M. F. R. Pereira, Bimetallic catalysts supported on activated carbon for the nitrate reduction in water: Optimization of catalysts composition, *Appl. Catal., B*, 2009, **91**, 441–448.

142 Z. Wang, S. D. Young, B. R. Goldsmith and N. Singh, Increasing electrocatalytic nitrate reduction performance by tuning adsorption through PtRu alloying, in *ECS Meeting Abstracts*, IOP Publishing, 2020, vol. MA2020-02, p. 3267.

143 Z. Wang, D. Richards and N. Singh, Recent discoveries in the reaction mechanism of heterogeneous electrocatalytic nitrate reduction, *Catal. Sci. Technol.*, 2021, **11**, 705–725.

144 P. H. van Langevelde, I. Katsounaros and M. T. Koper, Electrocatalytic nitrate reduction for sustainable ammonia production, *Joule*, 2021, **5**, 290–294.

145 N. Barrabés and J. Sá, Catalytic nitrate removal from water, past, present and future perspectives, *Appl. Catal., B*, 2011, **104**, 1–5.

146 Z. Wang, E. M. Ortiz, B. R. Goldsmith and N. Singh, Comparing electrocatalytic and thermocatalytic conversion of nitrate on platinum-ruthenium alloys, *Catal. Sci. Technol.*, 2021, **11**, 7098–7109.

147 S. D. Ebbesen, B. L. Mojet and L. Lefferts, Effect of pH on the nitrite hydrogenation mechanism over Pd/Al$_2$O$_3$ and Pt/Al$_2$O$_3$: Details obtained with ATR-IR spectroscopy, *J. Phys. Chem. C*, 2011, **115**, 1186–1194.

148 R. Yang, L. Mei, Y. Fan, Q. Zhang, H. G. Liao, J. Yang and Z. Zeng, Fabrication of liquid cell for in situ transmission electron microscopy of electrochemical processes, *Nat. Protoc.*, 2023, **18**, 555–578.

149 Q. Zhang, J. Ma, L. Mei, J. Liu, Z. Li, J. Li and Z. Zeng, In situ TEM visualization of LiF nanosheet formation on the cathode-electrolyte interphase (CEI) in liquid-electrolyte lithium-ion batteries, *Matter*, 2022, **5**, 1235–1250.

150 Y. Zhang, R. Yang, H. Li and Z. Zeng, Boosting electrocatalytic reduction of CO$_2$ to HCOOH on Ni single atom anchored WTe$_2$ monolayer, *Small*, 2022, **18**, 2203759.

151 Y. Li, G. Tian, B. Chen and J. Liang, Self-templating construction of flower-like mesoporous magnesium silicate composites from sepiolite for high-efficiency adsorption of aflatoxin B1, *Sep. Purif. Technol.*, 2022, **291**, 120953.

152 Y. Wang, C. Wang, M. Li, Y. Yu and B. Zhang, Nitrate electroreduction: mechanism insight, in situ characterization, performance evaluation, and challenges, *Chem. Soc. Rev.*, 2021, **50**, 6720–6733.

153 H. Liu, X. Jia, A. Cao, L. Wei, C. D'agostino and H. Li, The surface states of transition metal X-ides under electrocatalytic conditions, *J. Chem. Phys.*, 2023, **158**, 124705.

154 W. Yang, Z. Jia, B. Zhou, L. Wei, Z. Gao and H. Li, Surface states of dual-atom catalysts should be considered for analysis of electrocatalytic activity, *Commun. Chem.*, 2023, **6**, 6.

This journal is © the Partner Organisations 2023

Inorg. Chem. Front., 2023, **10**, 4610–4631 | **4631**